Bachelor thesis

Design, test and improvement of a vortex flow turbine for developing countries

Lucerne University of Applied Sciences and Arts

Study program Energy Systems Engineering

Author:	Ritz Jonas
Supervisor:	Dr. Deniz Sabri
Industry partner:	Dr. Richard Vögeli
Company:	AquaZoom AG

Horw, Lucerne University of Applied Sciences and Arts

04th of January 2021

Bachelor's thesis at the Lucerne School of Engineering and Architecture

Title	**Design, test and improvement of a vortex flow turbine for developing countries**
Student	**Ritz, Jonas**
Bachelor's degree program	**Bachelor in Energy Systems Engineering**
Semester	**fall semester 20**
Lecturer	**Deniz, Sabri**
External examiner	**Schlienger, Joel**

Abstract German

Gegenstand der vorliegenden Bachelor-Arbeit wird ist die Entwicklung einer Wirbelstromturbine für Entwicklungsländer, welche aus Schrottteilen hergestellt werden kann. Ziel ist es, der lokalen Bevölkerung von Drittweltländern eine Montageanleitung zu geben, damit sie die Wirbelstromturbine selbst bauen können, um den erzeugten Strom für ihren täglichen Bedarf zu nutzen.

In dieser Bachelor-Arbeit wird die Konstruktion der Wirbelstromturbine vorgestellt, welche dann genutzt wird, um Tests durchzuführen und weitere Konstruktionsverbesserungen zu untersuchen. Die hergestellte Wirbelstromturbine wurde dann in einem Wasserkanal getestet, um einen Einblick in die Gesamtleistung und Funktionalität der Wirbelstromturbine zu erhalten.

Die Wirbelstromturbine wurde im HSLU-Labor aus Schrottteilen hergestellt, die auf dem Schrottplatz gesammelt wurden oder die sonst von Unternehmen weggeworfen worden wären. Anschließend wurde die Wirbelstromturbine in einem Wasserkanal im HSLU-Labor getestet.

Die Ergebnisse zeigen, dass die Drehzahl, welche am Generator der Wirbelstromturbine im Leerlauf erreicht werden kann, ungefähr 950 $min{-}1$ beträgt. Darüber hinaus ergab die Prüfung des Generators, dass das Gerät mit einer Drehzahl von etwa 900 $min{-}1$ betrieben werden muss, um eine Überspannung zu erzeugen. Die Bachelor-Arbeit schlägt weitere Optimierungen der Wirbelstromturbine vor zum Bespiel, das Testen der Turbine mit der Simulation eines Innenwiderstands am Generator und eine Optimierung der Form und Geometire der Rotorschaufeln.

Abstract English

This bachelor thesis investigates the development of a vortex flow turbine applicable for developing countries, which can be built out of scrap parts. The aim is to provide an assembly instruction to the local population of third world countries, so that they can construct the vortex flow turbine by themselves to use the generated power for their daily needs.
This thesis presents the construction of the vortex flow turbine to perform tests and examines further construction improvements. The manufactured vortex flow turbine then is tested in a water channel to gain an insight into the overall performance and functionality of the vortex flow turbine.

The vortex flow turbine has been constructed in the HSLU laboratory out of scrap parts, that have been collected from scrap yards or that would have been thrown away by companies otherwise. Afterwards, the vortex flow turbine has been tested in a water channel in the HSLU laboratory.

The results indicate that the rotational speed, which can be attained at the generator of the vortex flow turbine under no-load conditions is approximately 950 $min{-}1$. Furthermore, the testing of the generator revealed that the device must be operated at a rotational speed of around 900 $min{-}1$ to generate an excess voltage. The thesis suggests for further optimizations of the vortex flow turbine to test the turbine with simulating an inner resistance at the generator and to further improve the shape and geometry of the rotor blades.

Place, date Horw, 04th of January 2021

Table of Contents

1. Introduction

The thesis continues the industrial project “Development of a vortex flow turbine for developing countries” (Ritz, 2020). In that project a vortex flow turbine for developing countries has been designed. The thesis now deals with the construction and the testing of the vortex flow turbine designed in the industrial project.

1.1 Starting situation

The company AquaZoom AG launched the project “Development of a vortex flow turbine for developing countries” (Ritz, 2020), to provide people of third world countries with an instruction on how to build a rudimentary vortex flow turbine out of scrap parts. AquaZoom AG is a company, which was founded in Switzerland and was originally known under the name Verde Renewables AG. The company has the aim to ensure access to affordable, reliable and sustainable energy for inhabitants of third world countries.

This bachelor thesis is a follow up from the industrial project “Development of a vortex flow turbine for developing countries” by Jonas Ritz, June 2020 at Lucerne university of applied science. The industrial project had the aim to draft and design a cheap vortex flow turbine out of scrap parts, which is applicable to developing countries and can be completely constructed by the locals themselves. The bachelor thesis will document the implementation of the construction, the tests in the laboratory and further possible improvements of the vortex flow turbine.

The target group for the constructed vortex flow turbine in the thesis are people from third world countries who live in villages located next to rivers and have a desire for electricity. The idea is to provide an assembly manual and a video which shows the construction of the vortex flow turbine, in order that the locals can construct the turbine by themselves. Everything was designed out of scrap parts, to make it affordable for the target group.

Vortex flow turbines can be operated with a low head and a small volume flow rate. Therefore, their field of application is next to rivers. By leading a waterflow tangentially to the inlet of a circular basin a swirl occurs. The rotation speed of a swirl increases by decreasing the radius in radial direction, which leads to a drop in pressure at the centre. If the pressure falls below atmospheric pressure, the water will be sucked into the outlet and a proper vortex will be created. By placing a rotor in the centre of this vortex, the rotor will start rotating. The rotational moment of the rotor then can be used to produce electricity by connecting the rotor to a generator.

1.2 Aim and objectives

The goal of the thesis is to construct, test and improve the vortex flow turbine, which was designed in the previous industrial project. The thesis aims to prove the functionality and feasibility of the designed vortex flow turbine and proposes further enhancements after the laboratory tests. The objectives are to construct a vortex flow turbine, which must be able to produce approximately 60W and can be fully produced out of scrap parts by the local population of third world countries.

The target in the end is to provide the people of third world countries with an assembly manual in written and visual form, with the purpose that the vortex flow turbine can be constructed by people needing it, out of available scrap parts from their local scrap yards. The produced electricity from the vortex flow turbine then can cover local electricity demands, such as loading phones or providing homes with an electrical lighting.

1.3 Structure of report

The first part of the thesis deals with the improvement of the rotor designed in the industrial project (Ritz, 2020). The outcome of the industrial project was that the construction of the rotor is too elaborate. Therefore, the thesis starts with the optimization and simplification of the rotor design.

The second part of the thesis covers the acquisition of the scrap parts and the manufacturing of the vortex flow turbine. A table lists the scrap parts, which had to be collected and the place where the parts have been acquired from. The chapter “Assembly manual” describes theoretically how the vortex flow turbine can be constructed and the chapter “Construction of the vortex flow turbine” documents the actual construction process.

The third part describes the laboratory experiments performed on the vortex flow turbine and the results gained out of the tests. This section focuses on attaining an insight into the performance of the vortex flow turbine and provides potential improvements for the last part of the thesis.

The fourth part indicates improvements, which have been performed during the construction process of the vortex flow turbine and shows the advantages compared to the designed vortex flow turbine from the industrial project (Ritz, 2020).

The last section of the thesis evaluates the findings of the laboratory experiments and proposes further adjustment and improvements. The part shows how the vortex flow turbine can be further optimized to achieve a better performance.

2. Methodology

In the industrial project “Development of a vortex flow turbine for developing countries” (Ritz, 2020), a vortex flow turbine for developing countries was dimensioned and designed. The project aim was to design a vortex flow turbine, which can be produced out of scrap parts and can be constructed with rudimentary tools by people living in third world countries. This thesis continues this project and deals with the practical part such as the construction and the testing of the previous designed vortex flow turbine. The thesis includes the collection of the necessary scrap parts, the physical construction of the vortex flow turbine and the testing phase of the turbine in the HSLU laboratory.

In a first step the necessary scrap parts for the construction of the vortex flow turbine will be collected. To have an overview of the needed scrap parts, a checklist is created, which assists the collection process by illustrating which parts are needed, what their dimension are, where they can potentially be found and if they are already procured. After completing the checklist, suitable companies and scrap yards can be contacted and visited to collect the scrap parts. In the end of the collection process, all scrap parts should be attained and the next step, the construction of the vortex flow turbine can be started.

After having attained all the necessary scrap parts, the construction of the vortex flow turbine can be planned. This planning mainly consists of creating an assembly manual. It describes the construction process of the vortex flow turbine step by step. The assembly manual then serves as a supporting material during the construction of the vortex flow turbine. If a proper manufacturing instruction is created, the scrap parts can be processed and then connected to the final vortex flow turbine. During the construction of the vortex flow turbine, the process will be filmed and pictures will be taken to create a visual assembly instruction in form of a video. The assembly instruction then will be uploaded on the web page of the company AquaZoom AG (www.aquazoom.com) and will be published in form of an open-source video.

When the construction of the vortex flow turbine is completed, the testing phase can be initiated. In a first step the car alternator will be tested. The outcome of the test should be the amount of electrical power a car alternator can produce by being operated with a certain rotational from the developed vortex flow turbine. Furthermore, tests with the final construction of the vortex flow turbine will be executed. In these tests first insights into the performance of the vortex flow turbine can be attained and further optimizations and adjustments can be performed accordingly. Also, the potential amount of electrical power delivered by the vortex flow turbine will be measured and analysed.

3. Rotor optimization

The conclusion of the industrial project (Ritz, 2020) proposed that the rotor should be improved as its design requires an elaborate construction process. Therefore, the first step of the thesis is to reduce the rotor design in its complexity by keeping the design as efficient as possible. The focus on the simplification of the rotor design lies on reducing the number of blades and adjusting the geometry and shape. The target is to find a compromise between designing an efficient construction and keeping a rudimentary design.

3.1 Effect of the number of blades

The first part which must be analyzed in terms of the rotor optimization is to reduce the number of rotor blades from the rotor developed in the industrial project (Ritz, 2020). The target of a reduction in rotor blades is to reduce the complexity of the rotor design and to allow a simple construction process of the rotor. The following section discusses the effect of the number of blades of a rotor on the performance and efficiency of the turbine.

3.1.1 Test to figure out which number of blades is the most suitable

Sritram and Suntivarakorn, (2019) discuss the testing of rotors with different number of blades and the resulting deviations in power output and occurring torque on the rotor. The test has been performed to analyze, which number of blades between 2 to 7 result in the highest torque and deliver the highest electrical power.

To perform the experiments, 6 rotors differing from 2 to 7 blades have been constructed. Nevertheless, the 6 rotors only deviated in the number of blades and kept the same dimensions with a diameter of 0.45m and a height of 0.32m. The rotors have been connected to a power generation system and were operated under a volume flow rate of $0.06 m^3 s^{-1}$. The load in the rotor has been changed by increasing the load in steps of 25W from 0 to 100W.

During the operation of the test, the water head, the revolution of the rotor, the voltage and the electric current were measured. With the attained values for the water head, the revolution of the turbine, the voltage and the current, the torque and the electrical power for the different rotors have been calculated by applying the formulas presented below (See abbreviations in section 13). The target was to analyze, which number of blades results in the highest torque and electrical power output and therefore should be chosen for the rotor design.

Hydraulic power

$$P_{hydraulic} = \rho \cdot g \cdot Q \cdot H$$

Electrical power

$$P_e = U \cdot I$$

Moment

$$M = \frac{60 \cdot P_{hydraulic}}{2 \cdot \pi \cdot N}$$

Efficiency

$$\eta = \frac{P_e}{P_{hydraulic}}$$

3.1.2 Results of the experiment

The outcome of the test was that the highest torque yields at 5 rotor blades (see figure 1). Furthermore, 5 blades also lead to the highest torque over the whole loads ranging from 0 to 100W. Therefore, it can be concluded that the number of blades, which should be targeted for the design of the rotor are 5 blades.

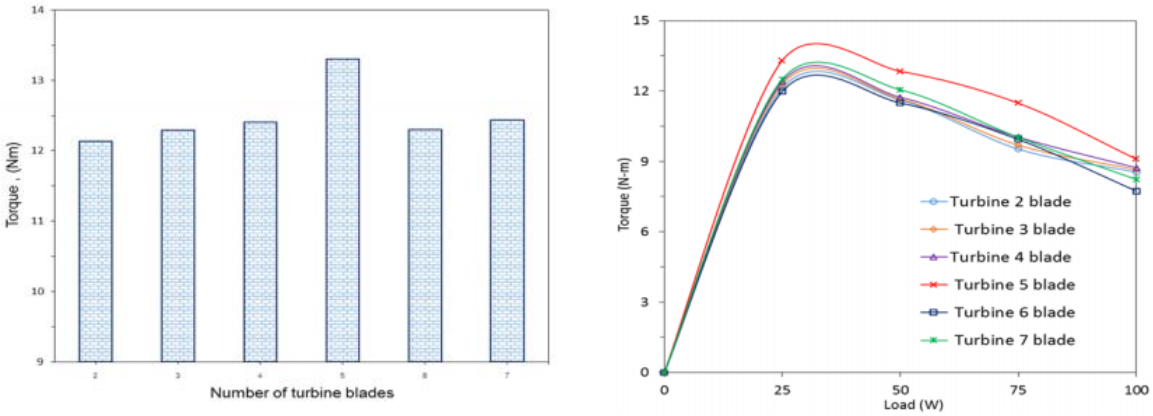

Figure 1 Torque attained at different turbine blade numbers

The experiment showed that the surface area, which encountered water was increasing up to 5 blades, which lead to a higher torque. After exceeding the number of 5 blades, the distance between the blades decreased, which resulted in a decrease in impact of water flow on the blades. In figure 2 the effect of the number of blades on the amount of water flow received on the blades can be seen.

Furthermore, with 6 and 7 blades the water flowing through the outlet generated a resistance on the following blades (see figure 2). This resistance occurred due to the leaving water flow, which resulted in a decrease on the exerted torque on the blades.

The number of 5 blades exploits the water flow on the blades efficiently and generates the highest torque. Therefore, it can be concluded that the number of blades chosen for the rotor should be 5 blades.

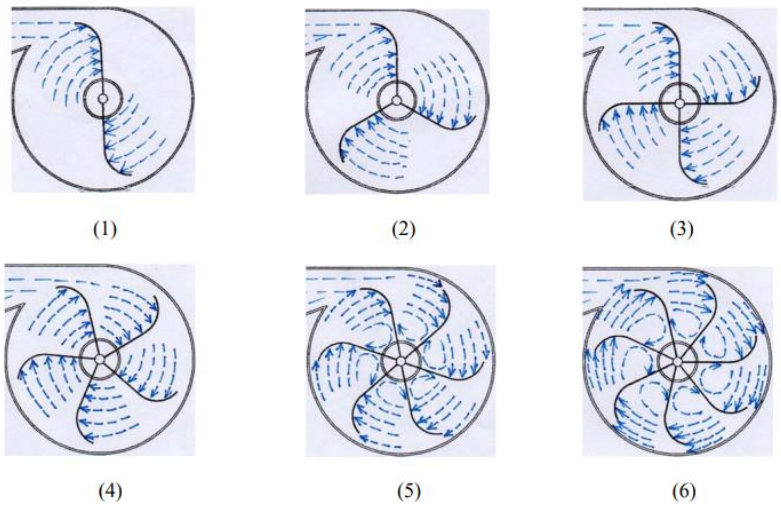

Figure 2 Water flow received by different number of blades

3.2 The effects of turbine baffle plates on the efficiency

Having discussed the effect of number of blades on the efficiency of the turbine, the geometry of the rotor blades also influences the turbines performance. The following section analyzes the effect of baffle plates on the efficiency of the rotor.

Sritram and Suntivarakorn, (2019) have raised the question of which percentage of covering yields the highest torque and electrical power. Furthermore, they tested if non baffle plates, only top baffle plates or top and bottom baffle plates yield better results. The target was to analyze if the efficiency increases by adding baffle plates to the blades of the rotor and which percentage of covering the geometry with baffle plates will lead to the highest performance.

3.2.1 Ideal percentage of covering the baffle plates

After finding out that 5 blades lead to the highest torque, an experiment was carried out with rotors with 5 blades but different percentages of baffles covering the blade geometry. The figure 3 shows the different baffle plates, which have been tested: No baffle, Case A 25% covered, Case B 50% covered, Case C 75% covered, Case D 100% covered.

The CFD program was used in their analysis to find out which proportion of baffle receive the highest efficiency. The outcome of the study was that Case B with 50% leads to the highest efficiency. Therefore, a baffle plate which covers approximately 50% of the rotor geometry leads to the highest performance of the turbine and should be targeted.

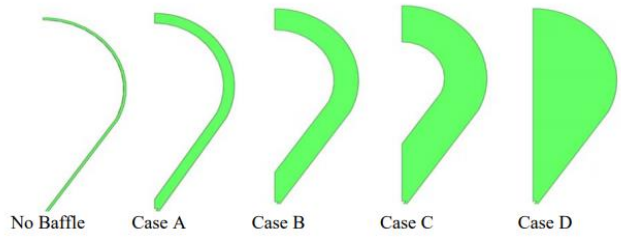

Figure 3 Different baffle plates

3.2.2 Amount of baffle plates

After having figured out which proportion of baffle plate is the most efficient, it had to be determined how many baffle plates per blade leads the best results. The following cases have been tested by Sritram and Suntivarakorn, (2019): Case 1 turbine blades with no baffle plates; Case 2 turbine blades with top baffle plates; and Case 3 turbine blades with top and bottom baffle plates (see figure 4). The different cases have been tested to analyze which amount of baffle plates leads to the highest performance of the rotor. The experiments were operated under a volume flow rate of $0.06m^3s^{-1}$ and the resulting torque and power outputs were measured.

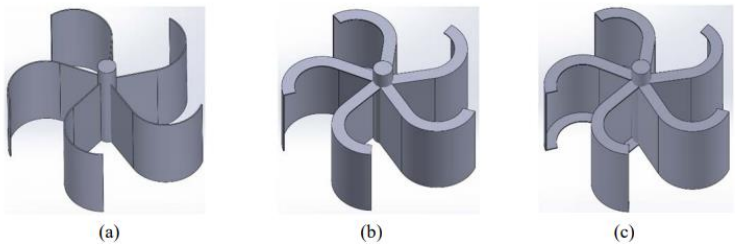

Figure 4 a) Turbine with baffle plates b) Turbine with top baffle plates c) Turbine with top and bottom baffle plates

3.2.3 Results of the test

The test performed in the study (Sritram & Suntivarakorn, 2019) lead to the result that a flow rate of $0.06m^3s^{-1}$ the case 3 with baffle plates on top and on bottom result in a higher torque than case 1 and 2 (see figure 5). The reason why the highest torque resulted in case 3 is because the baffle plates obtain a higher water mass on the surface of the rotor blade, which leads to a higher torque. Nevertheless, it can be observed that case 3 did not yield in a much higher output of electrical power than case 2.

In the end it can be concluded that adding baffle plates to the rotor design leads to an increase of the performance of the rotor. Therefore, in the scope of this project it is worth considering adding baffle plates to the final design of the rotor.

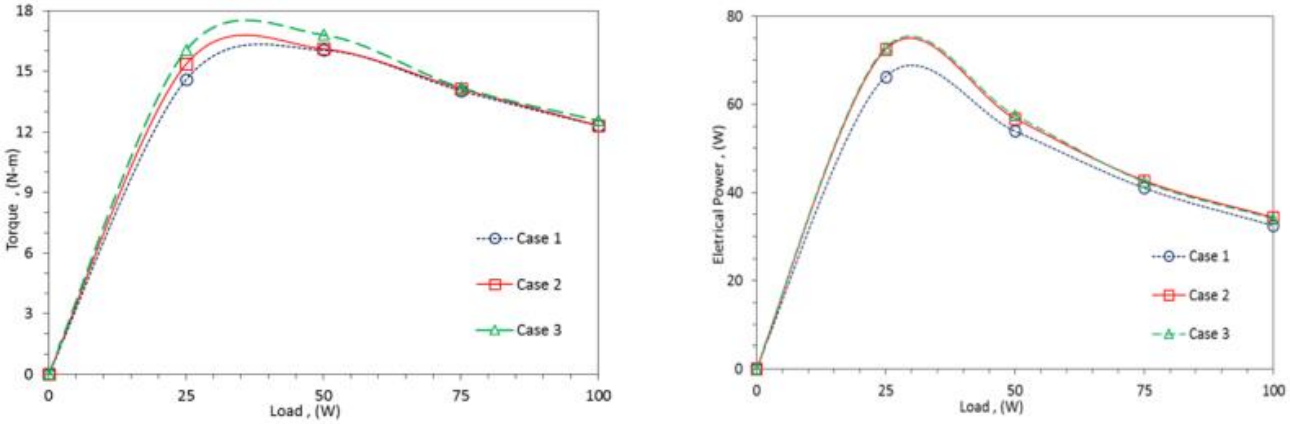

Figure 5 Torque and electrical power at turbine

3.3 Design adjustments

Having observed and analyzed the test results of the study by Sritram and Suntivarakorn, (2019), conclusions for the final design of the rotor can be drawn. The performed tests delivered data, which recommends the optimal number of blades and the effect of baffle plates on the rotor design.

It can be concluded that a rotor containing 5 blades yields the highest torque (Sritram & Suntivarakorn, 2019). This is the case because the distance between the blades causes an effective exertion of water flow on the surface of the blades. Therefore, to reach the highest torque and the highest power output, the rotor should contain 5 rotor blades.

The case 3 with top and bottom baffle plates lead to a higher torque than case 2 only top baffle plates and case 1 no baffle plates. Therefore, adding baffle plates on top and bottom of a rotor leads to the highest rotor performance. Furthermore, the baffle plates should cover around 50% of the rotor blade geometry to reach the highest performance. To achieve the most efficient rotor design, a rotor with top and bottom baffle plates which cover approximately 50% of the rotor blade geometry should be designed.

Nevertheless, the bachelor thesis does not primarily deal with the construction of a vortex flow turbine with an optimal efficiency, but rather focuses on the construction of a simple and cheap vortex flow turbine. Therefore, a compromise between an efficient and a rudimentary construction must be found.

3.4 Redesigning of the rotor

After having collected data considering the effect of the blade number and the baffle plates on the performance of the rotor, the rotor designed in the industrial project (Ritz, 2020) can be simplified and adjusted in its construction.

Two rotors have been designed, one focusing on providing the most rudimentary design possible and one focusing on an efficient but still simple design. Both rotors will be constructed and tested. The target is to see the difference in their performance and deciding, which rotor should be implemented in the end.

This section shows the rotor designed in the industrial project (Ritz, 2020) and elucidates the major problems with that rotor design. Furthermore, two rotors will be constructed which target a more rudimentary construction by still trying to achieve an efficient design.

3.4.1 Design from industrial project

The rotor designed in the industrial project (Ritz, 2020) had a height of 760mm and a diameter of 310mm. The middle of the rotor consisted of a pipe with a diameter of 254mm with 15 blades attached to it (see figure 6).

The design proposed 15 blades, which resulted in an elaborate welding effort and therefore was not that rudimentary in its construction. Therefore, the following rotor designs propose a simpler design by still focusing on reaching an efficient rotor construction.

Figure 6 Rotor design from industrial project

3.4.2 Changed rotor design option 1

To decrease the complexity of the rotor designed in the industrial project (Ritz, 2020), it was decided that the number of blades will be reduced to 5 blades instead of 15. Nevertheless, the height of 760mm and the diameter of 310mm was not adjusted, as the rotor dimensions were calculated in the industrial project (Ritz, 2020). Furthermore, the pipe of the rotor, which had the function of the axis, was replaced by a threaded rod, to allow a larger surface area of the blades by containing the same rotor diameter of 310mm.

Figure 7 Rotor with straight blades

3.4.3 Changed rotor design option 2

The second rotor design proposes a design with rounded rotor blades and with baffle plates attached to both ends (see figure 8). The second rotor alternative focuses on a more efficient design than on a rudimentary construction. Nevertheless, the dimensions with a radius of 310mm and a height of 760mm have been perceived. Also, the number of blades has been kept at 5 as it was proposed in section 3.1.2.

Figure 8 Rotor with rounded blades

To increase the efficiency and achieve a higher rotational speed, an option with rounded blades has been designed. The geometry (see figure 9) has been adopted from the article (Sritram & Suntivarakorn, 2019) and has been scaled to the required radius of 149mm accordingly (see figure 10). To simplify the construction of the blade's radius, the design has been changed from a proper radius to a geometry with four bends (see figure 9 & figure 10).

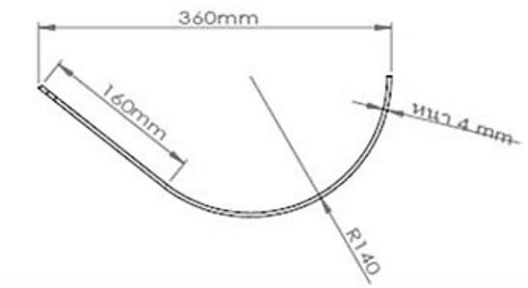

Figure 9 Blade geometry

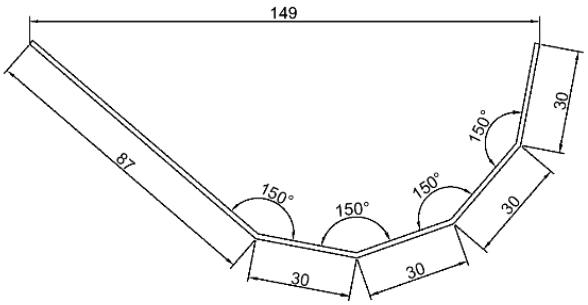

Figure 10 Adjusted blade geometry

To reach an optimum efficiency, baffle plates have been added on the top and bottom of the rotor. The baffle plates have been designed in order that they cover approximately 50% of the rotor geometry (see figure 11), as it has been suggested in section 3.2.1.

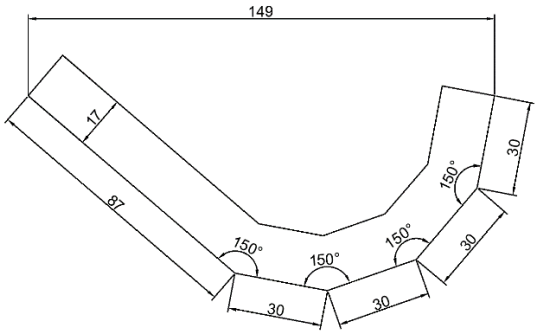

Figure 11 Baffle plate geometry

4. Procurement of scrap parts

In a first step, all scrap parts needed for the construction of the vortex flow turbine must be collected. To allow an organized procurement process, a checklist including a listing of all scrap parts with their dimensions is recommended. Furthermore, the amount of each scrap part and potential places where the specific parts can be found is crucial to keep track on. During the acquisition process under the column “Status” it can be actualized if the parts are already found and a constant overview of the acquired parts can be obtained.

The checklist serves as a supporting material during the first face of the project and prevents losing the overview of the status of the scrap parts. Furthermore, the acquisition process of the scrap parts gives a first overview if the vortex flow turbine was designed in a way that the procurement of the parts is straightforward. If all parts have been found and no specific part caused trouble in being acquired, a detailed description of the construction process of the vortex flow turbine can be created.

Scrap part	Used for	Amount	Dimension	Place to find	Status
Wooden pallet	Assembly group 1	1	145·800·1200	HSLU laboratory	OK
Oil barrel 200l	Assembly group 1	1	Ø585·880	MGB	OK
Wooden beam (front)	Assembly group 1	1	40·140·440	HSLU laboratory	OK
Wooden beam (side)	Assembly group 1	2	40·140·600	HSLU laboratory	OK
Wooden plate (front)	Assembly group 1	1	25·140·370	HSLU laboratory	OK
Wooden plate (side)	Assembly group 1	2	25·140·970	HSLU laboratory	OK
Wooden plate (lid)	Assembly group 1	1	25·370·620	HSLU laboratory	OK
Aluminum plate	Assembly group 1	1	1·370·495	HSLU laboratory	OK
Wooden screws	Assembly group 1	22	Ø4·50	HSLU laboratory	OK
Steel plate	Assembly group 1	4	2·40·100	HSLU laboratory	OK
Threaded rod	Assembly group 1	1	M10·1000	HSLU laboratory	OK
Threaded rod	Assembly group 1	1	M12·1000	HSLU laboratory	OK
Screws	Assembly group 1	8	M10·35	HSLU laboratory	OK
Nuts	Assembly group 1	8	M10	HSLU laboratory	OK
Bicycle wheel	Assembly group 2	1	Ø584	Radsport Zenger AG	OK
Motorcycle rim	Assembly group 2	1	16-inch	Garage Wenger	OK
Threaded rod	Assembly group 2	1	M12·1000	HSLU laboratory	OK
Nuts	Assembly group 2	4	M12	HSLU laboratory	OK
Steel plate	Assembly group 2	5	2·150·760	HSLU laboratory	OK
Aluminum plate	Assembly group 3	1	1.2·700·700	HSLU laboratory	OK
Screws	Assembly group 3	18	M4·15	HSLU laboratory	OK
Nuts	Assembly group 3	18	M4	HSLU laboratory	OK
Wooden plate	Assembly group 3	As needed	20·100·210	HSLU laboratory	OK
Car alternator	Final assembly	1		Automobile Franzen	OK
Nuts	Final assembly	4	M10	HSLU laboratory	OK
Nuts	Final assembly	4	M12	HSLU laboratory	OK
Inner tube	Final assembly	1		Garage Wenger	OK
Steel wire	Final assembly	1	Ø0.8·3000	HSLU laboratory	OK
Plastic bucket	Final assembly	1	Ø315·300	HSLU laboratory	OK

Table 1 Scrap parts

5. Assembly manual

After having collected all the necessary scrap parts, the construction of the vortex flow turbine can be started. To have a guideline while constructing the turbine, an assembly manual was created. The assembly manual simplifies the construction process and serves as a schematic way to prevent mistakes during the construction.

The manufacturing instruction divides the vortex flow turbine into three assembly groups and describes which scrap parts are needed for each assembly group, the dimensions of the necessary scrap parts, the tools needed to produce a specific group and includes a detailed instruction of the construction process.

The assembly manual is an adaption of the industrial project “Development of a vortex flow turbine for developing countries” (Ritz, J. (2020). The manufacturing instruction contains similar content as in the referenced project. As certain improvements and adaptions were performed on the vortex flow turbine, the assembly manual was slightly adjusted.

Figure 12 Vortex flow turbine

5.1 First assembly group

Necessary parts:

Position	Scrap part	Amount	Dimension
1	Wooden pallet	1	145·800·1200
2	Oil barrel 200l	1	Ø585·880
3	Wooden beam (front)	1	40·140·440
4	Wooden beam (side)	2	40·140·600
5	Wooden plate (front)	1	25·140·370
6	Wooden plate (side)	2	25·140·970
7	Wooden plate (lid)	1	25·370·620
8	Aluminum plate	1	1·370·495
9	Wooden screws	22	Ø4·50
10	Steel plate	4	2·40·100
11	Threaded rod	1	M10·1000
12	Threaded rod	1	M12·1000
13	Screws	8	M10·35
14	Nuts	8	M10

Table 2 Scrap parts first assembly group

Necessary tools: Saw, chisel, hammer, drill

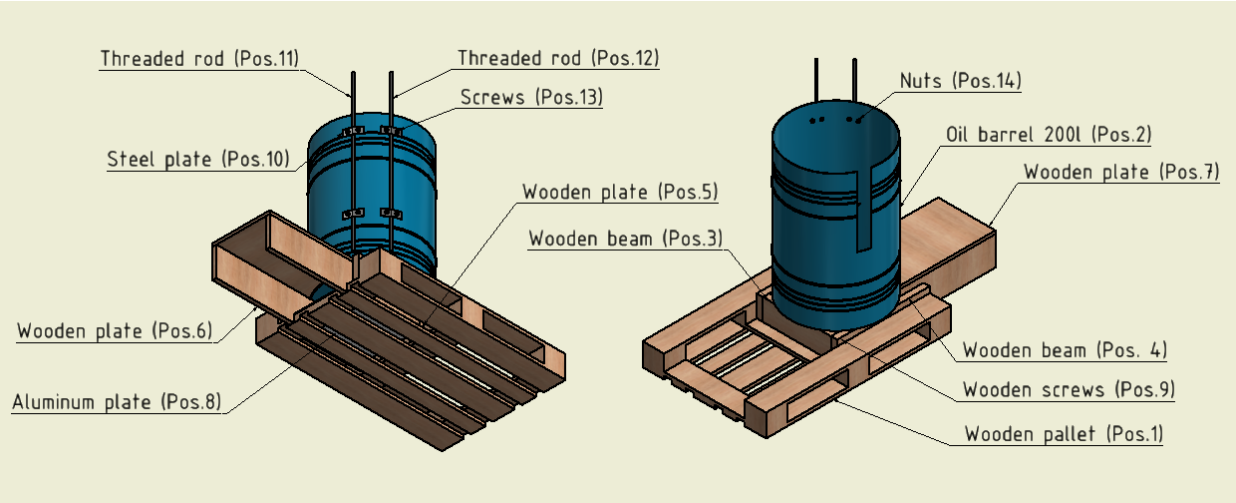

Figure 13 First assembly group

1. Take the oil barrel (Pos. 2) and saw a 27mm·450mm square in it around 10mm away from the outer diameter of the barrel (look at the technical drawing in the appendix). Then remove a roundel with a diameter of Ø240 from the oil barrel. A method is to use the chisel and the hammer to punch out the roundel. In the end drill 8 holes (position and dimension can be seen in the technical drawing in the appendix) in the oil barrel.

2. Take the two threaded rods (Pos. 11 & 12) and saw them to the length of 1000mm. Saw out 4 steel plates (Pos. 10) with the dimensions 2mm·40mm·100mm and drill two holes with a diameter of 11mm and a distance of 56mm between them. The threaded rods can be fixed through the 8 holes drilled in step 1 to the oil barrel, by clamping them between the oil barrel and the steel plates with the screws (Pos. 13) and the nuts (Pos. 14).

3. Take the three wooden plates (Pos. 5 & 6) and screw them together in the form of a u-profile. Afterwards screw the aluminum plate (Pos. 8) on the three wooden plates as a lid. Having connected the wooden plates and the aluminum plate, the construction can be screwed to the bottom of the 200l oil barrel. In the end, the wooden plate (Pos. 7) can be screwed on the extruding wooden plates (Pos. 6).

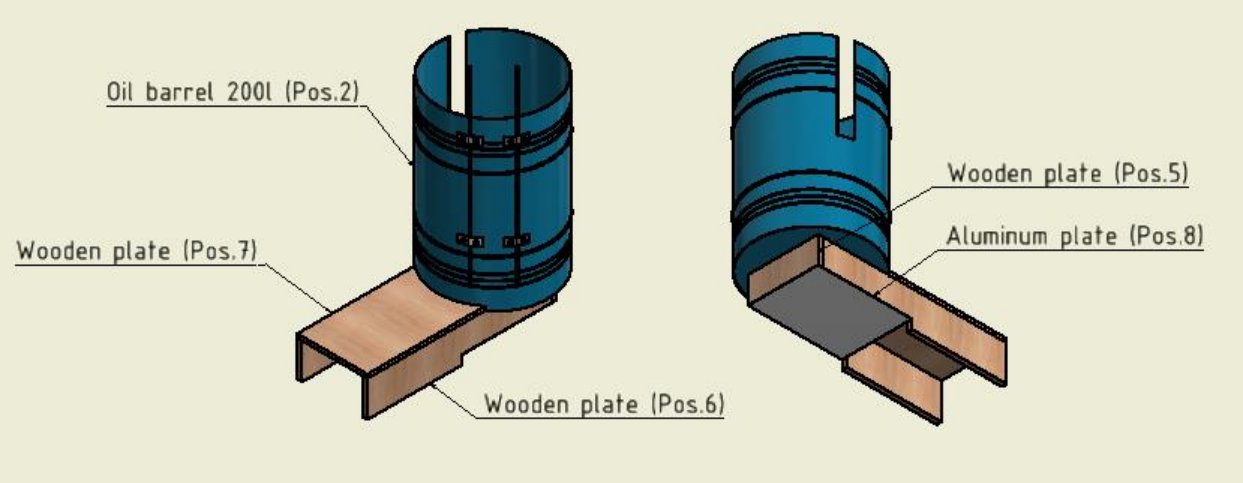

Figure 14 First assembly group without wooden pallet

4. Remove the middle part of the wooden pallet (Pos. 1) with a hammer. Afterwards screw the wooden beams (Pos. 3 & 4) on the wooden pallet (The position and dimensions of the wooden beams can be seen in the technical drawing in the appendix). As a last step, connect the oil barrel to the wooden beams with wooden screws.

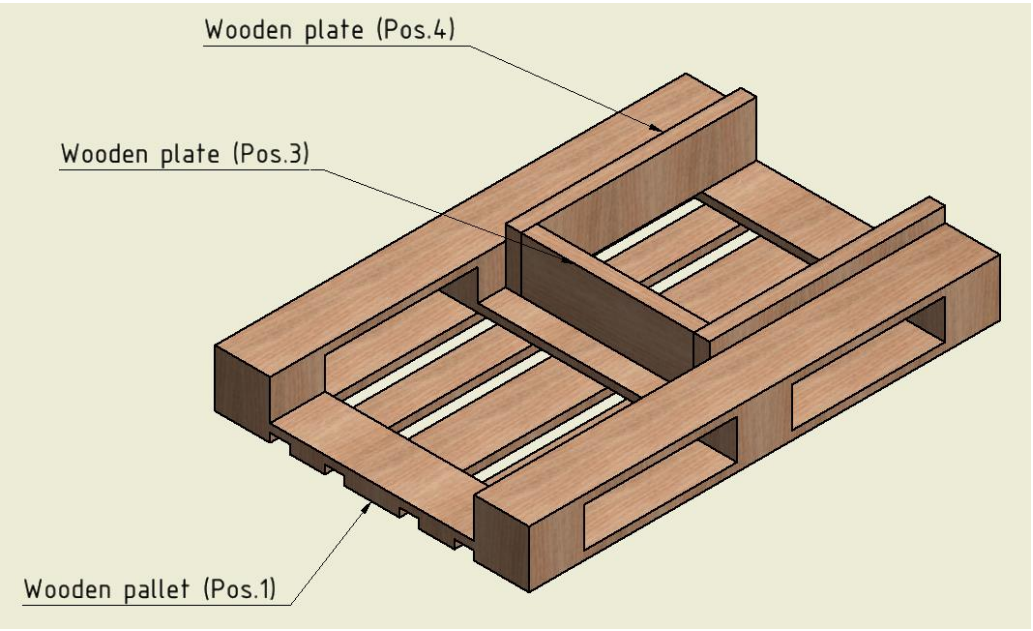

Figure 15 First assembly group wooden pallet

5.2 Second assembly group

Necessary parts:

Position	Scrap part	Amount	Dimension
1	Bicycle wheel	1	Ø584
2	Motorcycle rim	1	16-inch
3	Threaded rod	1	M12·1000
4	Nuts	4	M12
5	Steel plate	5	2·150·760

Table 3 Scrap parts second assembly group

Necessary tools: Welding equipment, saw, open-end wrench

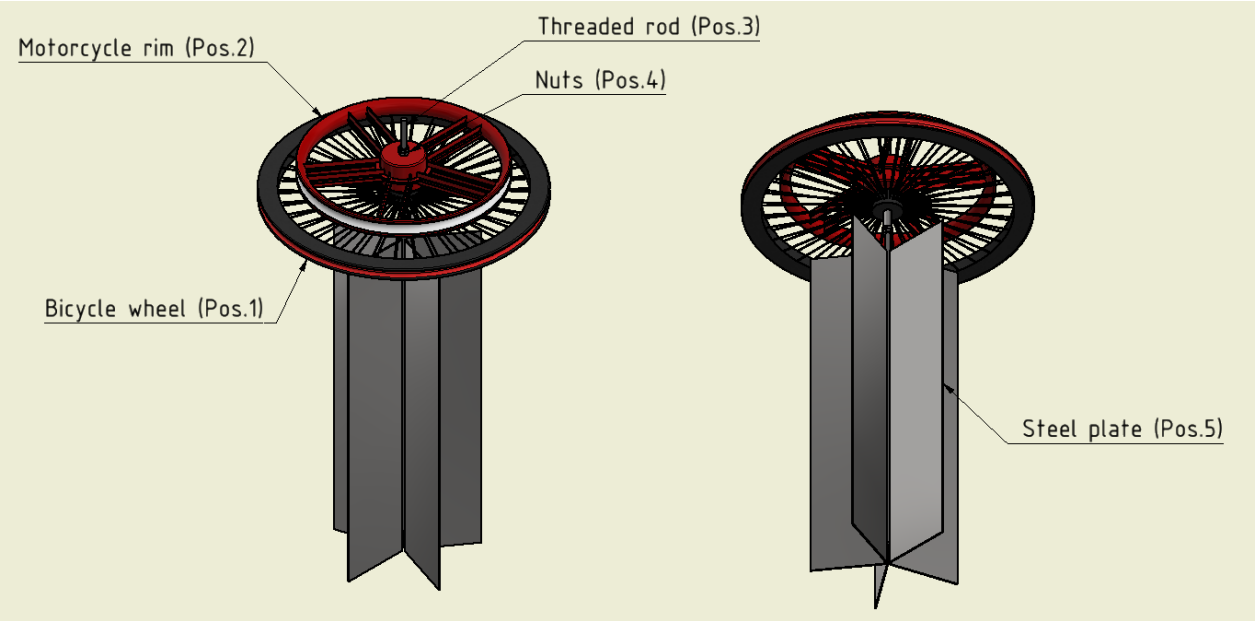

Figure 16 Second assembly group

1. Saw the 5 steel plates (Pos. 5) to the dimensions 2mm·150mm·760mm. Afterwards weld them to the threaded rod (Pos. 3) and let an angle of approximately 72° between the blades. The rotor should end up with a diameter of approximately 310mm.

2. Put the bicycle wheel (Pos. 1) and the motorcycle rim (Pos. 2) over the threaded rod (Pos. 3) and clamp them between the four nuts (Pos. 4). First fix two nuts on the threaded rod, then put the motorcycle rim and bicycle wheel on the threaded rod and in the end clamp everything with the two remaining nuts.

5.3 Third assembly group

Necessary parts:

Position	Scrap part	Amount	Dimension
1	Aluminum plate	1	1.2·295·309
2	Aluminum plate	2	1.2·96·429
3	Aluminum plate	1	1.2·126·430
4	Aluminum plate	1	1.2·304·430
5	Screws	18	M4·15
6	Nuts	18	M4
7	Wooden plate	As needed	20·100·210

Table 4 Scrap parts third assembly group

Necessary tools: Saw, hammer, drill, open-end wrench

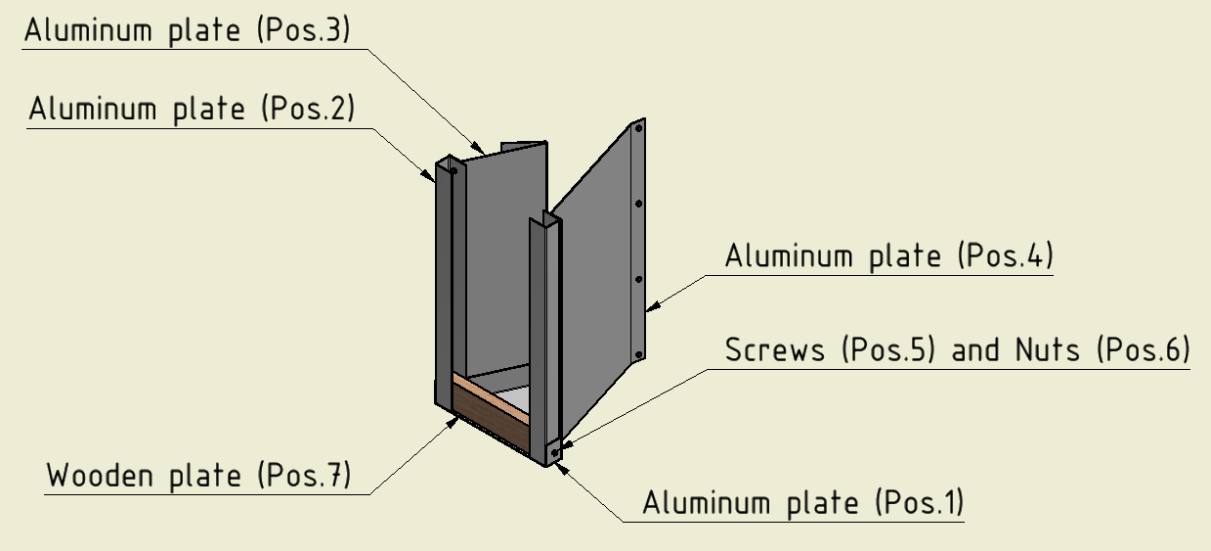

Figure 17 Third assembly group

1. Saw the aluminium plate into the desired shapes (The sheet metal design can be found in the technical drawing in the appendix).

2. Take the sheet metals (Pos. 1 & 2 & 3 & 4) and bend them to the required shapes (The bending shapes can be seen in the technical drawing in the appendix).

3. Connect the 5 sheet metals (Pos. 1 & 2 & 3 & 4) with the screws (Pos. 5) and the nuts (Pos. 6) according to figure 17.

4. The wooden plates (Pos. 7) can be placed in the conduct. The number of wooden plates depend on the area to which the inlet must be adjusted.

5.4 Final construction

Necessary parts:

Position	Scrap parts	Amount	Dimension
1	Car alternator	1	
2	Nuts	4	M10
3	Nuts	4	M12
4	Inner tube	1	
5	Steel wire	1	Ø0.8·3000

Table 5 Scrap parts final construction

Necessary tools: Open-end wrench

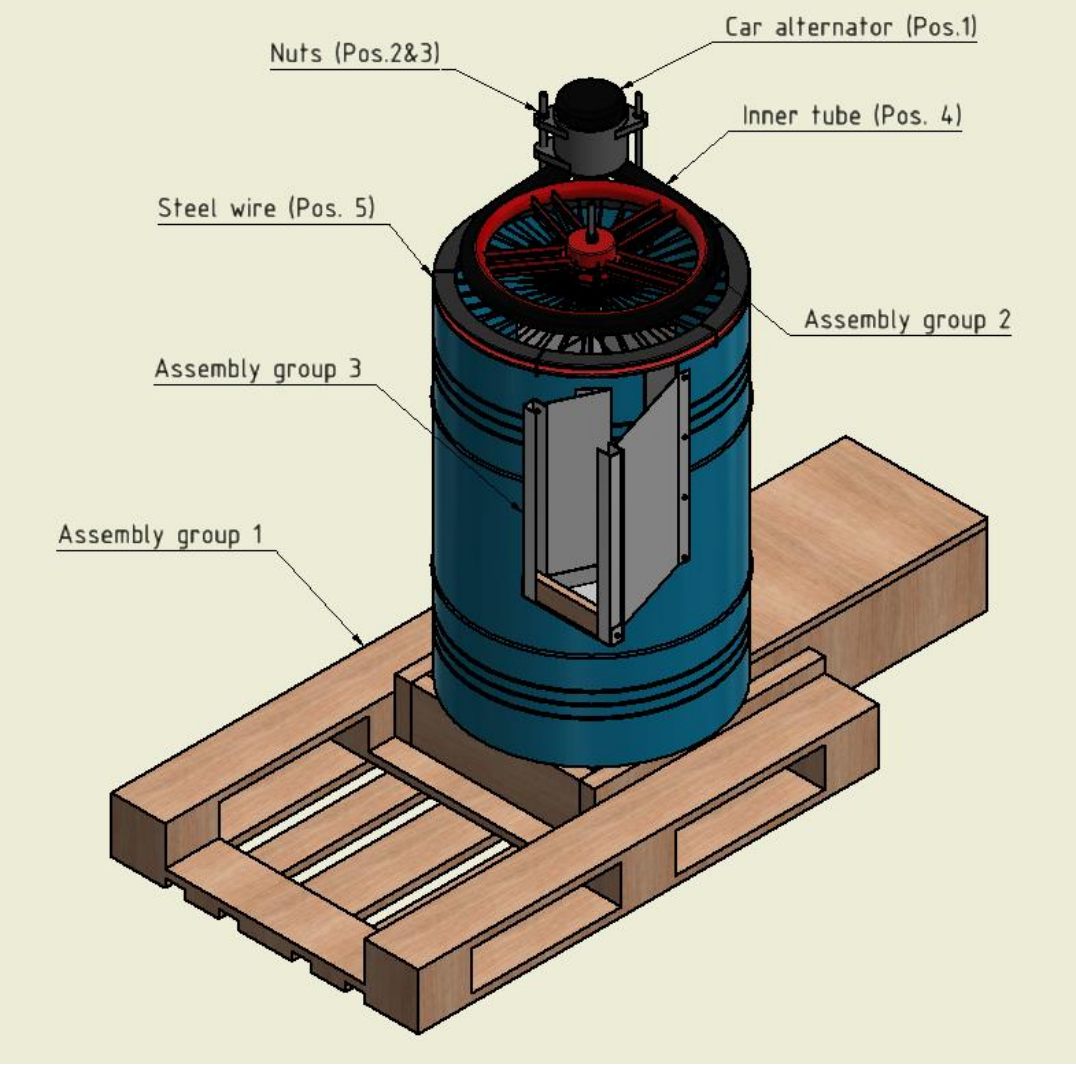

Figure 18 Final construction

1. The first assembly group and the second assembly group can now be connected by fixing the bicycle wheel with steel wire (Pos. 5) to the oil barrel.

2. Now the third assembly group can be screwed to the barrel. To change the volume flow rate, wooden plates can be placed in the gate of the third assembly group.

3. The car alternator (Pos. 1) can be fixed with four nuts (Pos. 2 & 3) on the threaded rods. In the end the inner tube (Pos. 4) can be put over the car alternator and the motorcycle rim.

6. Construction of the vortex flow turbine

After having attained the scrap parts and having written a theoretical manufacturing instruction, the physical construction of the vortex flow turbine can be started. The vortex flow turbine is divided into three assembly groups, which will be constructed first individually and, in the end, put together to the final vortex flow turbine. The manufacturing process of the vortex flow turbine will be conducted in the HSLU laboratory. The purpose of the physical construction of the turbine is to attain a prototype, which can be used to test the performance of the developed vortex flow turbine and to discover construction flaws, which can be eliminated in a further optimization process.

To show the inhabitants of third world countries the manufacturing process of the vortex flow turbine, the construction will be documented in written form and pictures of the manufacturing process will be taken to elucidate the performed construction steps. Furthermore, a video documentation of the manufacturing will be made. The purpose is to have a detailed written and visual instruction of the vortex flow turbine, so that the self-construction can be understood easily.

Table 6 shows all scrap parts, which were used for the final construction including their necessary amount and dimensions.

Scrap part	Used for	Amount	Dimension
Wooden pallet	Assembly group 1	1	145·800·1200
Oil barrel 200l	Assembly group 1	1	Ø585·880
Wooden beam (front)	Assembly group 1	1	40·140·440
Wooden beam (side)	Assembly group 1	2	40·140·600
Wooden plate (front)	Assembly group 1	1	25·140·370
Wooden plate (side)	Assembly group 1	2	25·140·970
Wooden plate (lid)	Assembly group 1	1	25·370·620
Aluminum plate	Assembly group 1	1	1·370·495
Wooden screws	Assembly group 1	22	Ø4·50
Steel plate	Assembly group 1	4	2·40·100
Threaded rod	Assembly group 1	1	M10·1000
Threaded rod	Assembly group 1	1	M12·1000
Screws	Assembly group 1	8	M10·35
Nuts	Assembly group 1	8	M10
Bicycle wheel	Assembly group 2	1	Ø584
Motorcycle rim	Assembly group 2	1	16-inch
Threaded rod	Assembly group 2	1	M12·1000
Nuts	Assembly group 2	4	M12
Steel plate	Assembly group 2	5	2·150·760
Aluminum plate	Assembly group 3	1	1.2·700·700
Screws	Assembly group 3	18	M4·15
Nuts	Assembly group 3	18	M4
Wooden plate	Assembly group 3	As needed	20·100·210
Car alternator	Final assembly	1	
Nuts	Final assembly	4	M10
Nuts	Final assembly	4	M12
Inner tube	Final assembly	1	
Steel wire	Final assembly	1	Ø0.8·3000
Plastic bucket	Final assembly	1	Ø315·300

Table 6 Scrap parts

6.1 Manufacturing first assembly group

To construct the first assembly group, the scrap parts according to table 7 are necessary. The construction of the group will be executed according to the created assembly manual in section 5. All dimensions can be seen in the technical drawings in the appendix.

Tools used: Saw, chisel, hammer, drill, open-end wrench

Scrap part	Amount	Dimension
Wooden pallet	1	145·800·1200
Oil barrel 200l	1	Ø585·880
Wooden beam (front)	1	40·140·440
Wooden beam (side)	2	40·140·600
Wooden plate (front)	1	25·140·370
Wooden plate (side)	2	25·140·970
Wooden plate (lid)	1	25·370·620
Aluminum plate	1	1·370·495
Wooden screws	22	Ø4·50
Steel plate	4	2·40·100
Threaded rod	1	M10·1000
Threaded rod	1	M12·1000
Screws	8	M10·35
Nuts	8	M10

Table 7 Scrap parts first assembly group

Step 1: Machining the oil barrel

The first step was to remove the lid and to saw the inlet into the 200l oil barrel. The lid was removed with a chisel and a hammer. To add the inlet, a square with the dimensions 27mm·450mm was sawed out (see figure 20).

The whole for the outlet resembled a bigger hurdle, as it had to be removed from the bottom of the barrel in its center. First a circle with a diameter of Ø254 was marked in the center of the barrel and then with chisel and hammer the rondel has been removed (see figure 21).

Figure 19 Oil barrel 200l

Figure 20 Removed lid

Figure 21 Removing rondel for outlet

Step 2: Adding the thread rods

To connect the threaded rods to the oil barrel, four plates were used to clamp the threaded roads between the barrel and the plates with screws. In a first step four plates (see technical drawing in the appendix) have been sawed out of a steel sheet with a thickness of around 2mm. The steel plates can also be bend slightly (see figure 22), to simplify the next step.

In the next step, 8 holes have been drilled into the oil barrel. The threaded rods can then be clamped between the oil barrel and the plates with screws (see figure 23). The alternator can be fixed, before the drilling of the holes, with 4 nuts to the treaded rods to ensure the precise position of the holes.

Figure 22 Bend steel plates

Figure 23 Threaded rods fixed to oil barrel

Step 3: Constructing the outlet

In the first step, 3 wooden plates have been screwed together with an angle of 90° between them and an aluminum plate has been screwed to the bottom of the wooden plates (see figure 24). The dimensions of the outlet can be seen in the technical drawing in the appendix.

The constructed outlet then has been screwed to the oil barrel (see figure 25). It must be considered that the opening of the outlet must be directed to the opposite direction of the inlet opening.

Figure 24 Outlet

Figure 25 Outlet fixed to oil barrel

Step 4: Machining the wooden pallet

The middle part of the wooden pallet was removed (see figure 26) and a with three wooden plates a frame was constructed as it can be seen in figure 27.

In the end, the oil barrel has been screwed to the frame of the wooden pallet. The outlet must be directed in the direction where the wooden frame is open.

Figure 26 Wooden pallet with removed middle

Figure 27 Wooden pallet with frame

Final first assembly group

The first assembly group has been finished and will be put together in the end with the two following assembly groups.

Figure 28 Final first assembly group

6.2 Manufacturing second assembly group

With the collected scrap parts from table 8, all necessary parts have been attained to start the construction of the second assembly group. As supporting material, the assembly manual from section 5 was used.

Tools used: Saw, welding equipment, open-end wrench

Scrap part	Amount	Dimension
Bicycle wheel	1	Ø584
Motorcycle rim	1	16-inch
Threaded rod	1	M12·1000
Nuts	4	M12
Steel plate	5	2·150·760

Table 8 Scrap parts second assembly group

Step 1: Welding rotor blades to the threaded rod

5 steel plates with a thickness of 2mm have been sawed to the dimensions 150mm·760mm. The blades then have been welded to the threaded rod M12·1000mm at an angle of around 72° between the blades.

Figure 29 Rotor during construction

Figure 30 Finished rotor

Step 2: Fixing bicycle wheel and motorcycle rim on rotor

In the second step the bicycle wheel and the motorcycle rim have been fixed on the rotor. The bicycle wheel and the motorcycle rim have been clamped between four nuts on the threaded rod (see figure 31).

Figure 31 Second assembly group

Final second assembly group

The second assembly group has been finished. To simplify the final construction, the second assembly group will be connected to the overall construction, after the third assembly group has been constructed.

Figure 32 Final second assembly group

6.3 Manufacturing third assembly group

In table 9 the necessary scrap parts for the manufacturing of the third assembly group can be seen. To manufacture the third assembly group in a structured way, the assembly manual from section 5 was used.

Tools used: Saw, hammer, drill, open-end wrench

Scrap part	Amount	Dimension
Aluminum plate	1	1.2·295·309
Aluminum plate	2	1.2·96·429
Aluminum plate	1	1.2·126·430
Aluminum plate	1	1.2·304·430
Screws	18	M4·15
Nuts	18	M4
Wooden plate	As needed	20·100·210

Table 9 Scrap parts third assembly group

Step 1: Sawing the plates into the specific forms and bending them

In a first step the aluminum plates were sawed into the required shapes (The sheet metal design can be found in the technical drawing in the appendix). Having sawed out the 5 sheet metals, they have been bent accordingly (see figure 33 and figure 34).

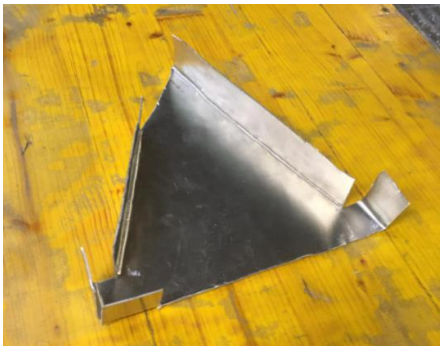

Figure 33 Bended ground plate

Figure 34 Bended conduct

Final third assembly group

The parts manufactured in the first step have been screwed together to the final assembly group (see figure 35). To stabilize the construction, a threaded rod has been added to connect the two walls as it can be seen in the picture below.

Figure 35 Final third assembly group

6.4 Final construction

After having manufactured the three assembly groups, the groups can be connected to the final vortex flow turbine. Additional parts which are necessary for the final construction of the vortex flow turbine can be seen in the table 10. Also, the final construction was performed according to the assembly manual from section 5.

Tools used: Open-end wrench

Scrap parts	Amount	Dimension
Alternator	1	
Nuts	4	M10
Nuts	4	M12
Inner tube	1	
Steel wire	1	Ø0.8·3000

Table 10 Scrap parts final construction

Step 1: Screwing the third assembly group to the first assembly group

In the first step the third assembly group has been connected to the first assembly group (see figure 36) by screwing the third assembly group to the inlet of the oil barrel.

Figure 36 Third assembly group connected to first assembly group

Step 2: Connecting the second assembly group to the first assembly group

The second assembly group has been put on the second assembly group, so that the bicycle wheel from the second assembly group lied on the oil barrel of the first assembly group (see figure 37). Afterwards, the bicycle wheel was connected to the oil barrel with steel wires.

Figure 37 Second assembly group connected to first assembly group

Final vortex flow turbine

After having connected the three assembly groups to each other, the remaining parts (see table 10) can be connected to the construction (see figure 38). The rotor was fixed to the threaded rods with four nuts. After the rotor was fixed to the construction, the inner tube was put over the car alternator and the motorcycle rim to connect them. As the turbine has been finished in its construction, the prototype of the vortex flow turbine can be used for the next step, the testing of the vortex flow turbine.

Figure 38 Final construction

7. Description of the video creation

A video of the construction process of the vortex flow turbine has been created, to provide a visual manufacturing instruction. The target was to offer, next to the written assembly manual, also a video which shows the actual construction of the vortex flow turbine.

Providing the option of a visual assembly manual, the population of third world countries attain the possibility to see how the vortex flow turbine can be constructed without reading or understanding the written assembly manual. The target group for the video are the population of third world countries who cannot read or have a better understanding, of the development of the vortex flow turbine, by watching an assembly instruction in form of a video.

The content of the video is a detailed assembly instruction, which follows a similar structure as the written assembly manual in section 5. The assembly video is divided into four main sections, the three assembly groups and the final assembly. Each section describes how the specific assembly groups must be constructed and which tools are necessary to perform the specific tasks. In the end of each section a video extract of the performed step is shown and represents a picture of the construction, which should be attained after the performed steps.

The program used for the creation of the video was the video editor program “Movavi”. It is a video editor, which allows the user to cut and to edit previously created videos. The overall construction process of the vortex flow turbine has been filmed, cut and subtitled with “Movavi”.

The final assembly video has been uploaded on the web page from the company AquaZoom AG (www.aquazoom.com). Therefore, the visual assembly manual can be accessed under the following link: “www.aquazoom.com”.

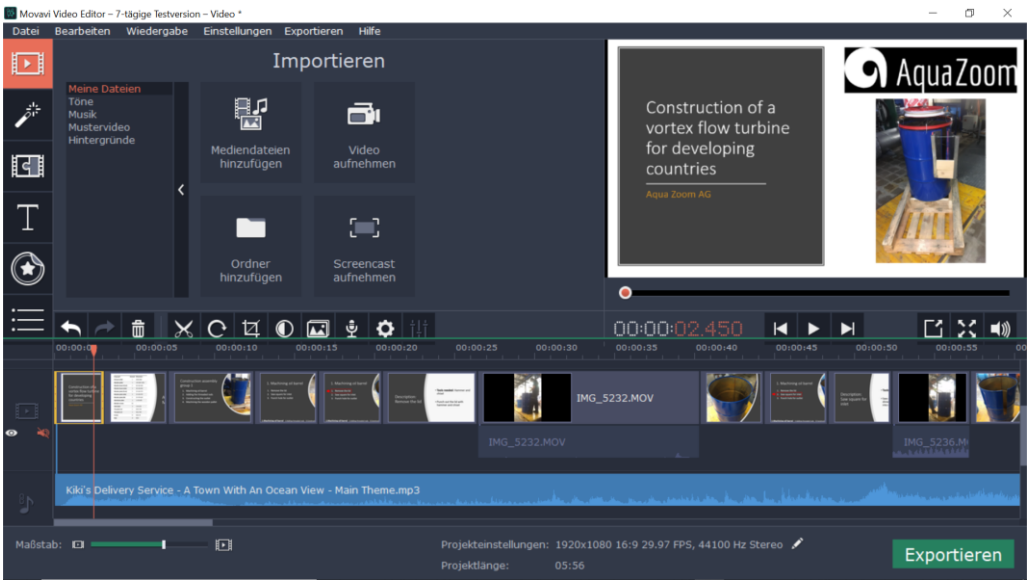

Figure 39 Movavi user interface

8. Testing of the vortex flow turbine

After having constructed the prototype of the vortex flow turbine, the testing phase can be started. The experiments will be performed at the HSLU laboratory. The target of the testing phase is to operate the developed vortex flow turbine under vortex turbine design conditions and to attain results of the overall performance and the power output of the car alternator. The results of the testing phase serve to discover construction flaws and to observe potential optimizations. In total 5 experiments will be conducted.

The first experiment which will be performed is the development of the vortex inside the vortex flow turbine. For the test the turbine, excluding the rotor, will be fixed in the water channel in the laboratory and a water flow will be conducted through the turbine. The target is to observe the developed vortex and to compare it optically with the calculated vortex in the industrial project (Ritz, 2020).

In the second test both rotor designs developed will be tested. Therefore, the vortex flow turbine will be put in the water channel and different volume flow rates will be provided to the vortex flow turbine. The goal of this experiment is to measure the rotational speed of the rotor and the car alternator.

The third experiment proposes the testing of the vortex flow turbine in the water channel, but with blocked sides to generate a height difference between inlet and outlet. The target of this test is to attain more realistic testing results then in the second experiment, as the testing conditions coincide more with the real-world application of the vortex flow turbine.

The fourth test is about testing the voltage output of the car alternator at different rotational speeds. To perform the experiment a testing fixture, with a motor attached to it, will be prepared and the car alternator will be connected to the testing fixture and coupled to the motor. With the motor then different rotational speeds will be applied and the attained voltages can be measured. The target of the experiment is to determine the minimum rotational speed, which must be provided by the vortex flow turbine to allow a power generation of the car alternator.

In the last experiment a wooden channel will be added to the front of the inlet. The wooden channel leads to an increase in the flow rate entering the vortex flow turbine and allows a testing of the turbine under more realistic operation conditions.

In the next subchapters the conducted experiments will be documented and examined in detail. Furthermore, conclusions will be drawn and further constructional changes and optimizations will be proposed.

8.1 Testing the shape of the vortex

The induced vortex in the vortex flow turbine provides the rotational movement for the rotor. In order that the rotor starts rotating, a proper vortex must be created. Therefore, the first test which has been performed was if the constructed vortex flow turbine creates the vortex, which was calculated in the industrial project (Ritz, 2020).

The target of the test was to examine if a proper vortex occurs when water flows with a volume flow rate of around $0.035 m^3 s^{-1}$ through the turbine or if the inlet or outlet of the vortex flow turbine must be adjusted in its dimensions. The expected vortex shape, which has been calculated in the industrial project (Ritz, 2020), can be seen in figure 40.

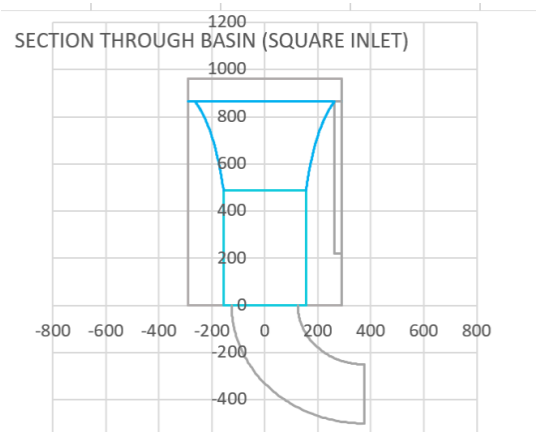

Figure 40 Calculated vortex shape

8.1.1 Testing procedure

Before the experiment can be performed, the first and second assembly group must be finished in its construction and be connected. The set-up needed to perform the test is the water channel at the fluid laboratory at the university of applied science in Luzern.

The vortex flow turbine, consisting of the first and second assembly group, can be placed into the water channel by using straps. The volume flow rate in the water channel can be regulated by adjusting the performance of the pump. It can then be observed if a desirable vortex occurs or if further adjustments on the inlet and outlet must be performed.

Figure 41 Experimental set-up

8.1.2 Performed experiment

To position the vortex flow turbine in the water channel, the turbine has been placed with the help of straps in the water channel and has been loaded with stones to prevent a flushing away of the turbine. The volume flow rate in the water channel was regulated to approximately $0.215 m^3 s^{-1}$, which led to a velocity in the water channel of around $0.2 m\ s^{-1}$.

The water channel in the laboratory did not allow to simulate a height difference between the inlet and the outlet of the vortex flow turbine. Therefore, with a gate placed behind the outlet, an under pressure has been created to generate a potential pressure difference between inlet and outlet. By slowly removing the gate at the outlet side of the turbine, while the water was flowing through the turbine, a vortex could be generated (see figure 42).

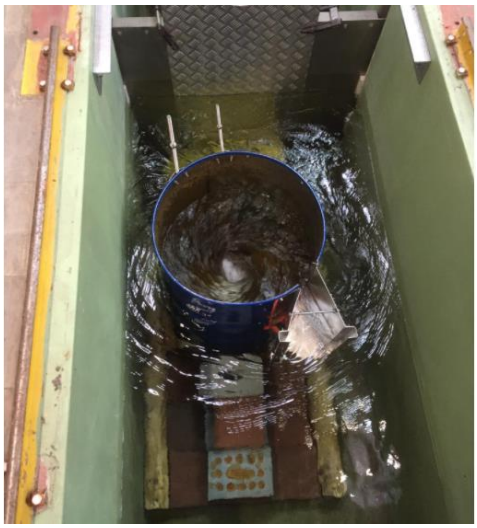

Figure 42 Developed vortex during experiment

8.1.3 Results

As it can be seen in figure 42, a proper vortex was generated and the experiment showed that the vortex flow turbine can be operated such that a proper vortex can be developed.

Nevertheless, to attain a vortex in the vortex flow turbine, a height difference between inlet and outlet must be created. To ensure the height difference in a river, a side-channel must be excavated (see figure 43). The side-channel must have the same width as the oil barrel of the vortex flow turbine, as it must be avoided that the water flow can pass aside the turbine. Having attained a proper vortex in the first experiment, further tests can be performed with the vortex flow turbine.

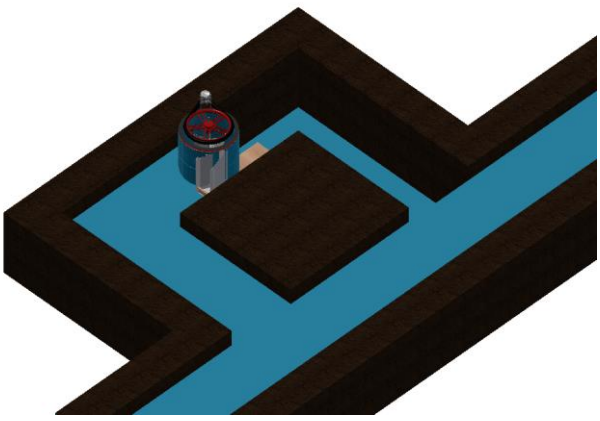

Figure 43 Operation of turbine under vortex turbine design conditions

8.2 Testing rotational speed of rotor and alternator

After having tested the development of the vortex inside the vortex flow turbine, the rotational speed of the rotor and the car alternator can be determined. Two different rotors have been constructed and will be tested and evaluated.

The target is to operate the vortex flow turbine under vortex turbine design conditions and to measure the rotational speed of the rotor and the car alternator. The test should show if the theoretical rotational speeds calculated in the industrial project (Ritz, 2020), can be achieved under vortex turbine design conditions. Furthermore, by dividing the rotational speed of the car alternator by the rotational speed of the rotor, it can be examined if the transmission ratio can be achieved or if further optimizations regarding the transmission material must be performed.

Figure 44 Rotor with straight blades

Figure 45 Rotor with rounded blades

8.2.1 Testing procedure

To perform the experiment, the first, the second and the third assembly group must be merged. The test will be conducted in the HSLU laboratory in the water channel. First the experiment will be performed for the rotor with straight blades (see figure 44) and afterwards the experiment will be repeated for the rotor with rounded blades (see figure 45).

The vortex flow turbine can be put into the water channel with the help of straps and can be fixed by placing stones on the wooden pallet of the vortex flow turbine to prevent a flash away of the turbine. The volume flow rate in the water channel will be increased from $0m^3s^{-1}$ to $0.5m^3s^{-1}$. As the area of the water channel is approximately $1m^2$, the speed in the channel ranges from $0ms^{-1}$ to $0.5ms^{-1}$. As the vortex flow turbine was developed for a river speed of $0.5ms^{-1}$, the focus of the experiment lies on measuring the rotational speed of the rotor and the car alternator at a volume flow rate in the water channel of $0.5m^3s^{-1}$. The rotational speed of the rotor and the car alternator were calculated in the industrial project (Ritz, 2020) and are supposed to be $200min^{-1}$ for the rotor and $1600min^{-1}$ for the car alternator. The rotational speed of the rotor and the car alternator can be measured with an oscilloscope. The set-up of the experiment can be seen in the figure 46 below.

Figure 46 Experimental set-up

8.2.2 Performed experiments

The vortex flow turbine has been put into the water channel with the help of two straps and fixed there by laying stones on the wooden pallet of the turbine. The test has been firstly performed for the rotor with straight blades and afterwards for the rotor with rounded blades. Nevertheless, the experiments have been conducted with the same volume flow rates for both rotor designs in the water channel. To observe the change of the rotational speed of the car alternator, at increasing volume flow rates, the volume flow rate inside the water channel has been varied in increasing steps of $50ls^{-1}$ from $200ls^{-1}$ to $500ls^{-1}$.

Afterwards, the rotational speed of the rotor and the car alternator have been measured with an oscilloscope. The following section discusses the results of the test with the rotor with straight blades.

8.2.3 Results straight blades

The results of the experiment with the rotor with straight blades can be seen in table 11. The lowest alternator rotational speed is at $410min^{-1}$ and the lowest rotor rotational speed is at $65min^{-1}$ and increases with a raising volume flow rate in the water channel. Nevertheless, in the graph 47, the increase in rotational speed starts to stagnate between a volume flow rate of $350l\ s^{-1}$ and $500l\ s^{-1}$. The stagnation of the rotational speed of the car alternator is illustrated in the graph 47 on page 36. Furthermore, friction losses caused a drop in the transmission ratio from the ideal value of 6.7 to around 6.3.

The targeted rotational speed of the car alternator of $1600min^{-1}$ has not been achieved. A reason may be that the potential difference has been created artificially as a pressure difference and not due to a difference in height, as it would be under real operation. Therefore, the experimental set-up has been adjusted (see section 8.3).

Volume flow rate supplied by pump [$\frac{l}{s}$]	**Alternator rotational speed [$\frac{1}{min}$]**	**Rotor rotational speed [$\frac{1}{min}$]**	**Transmission ratio [-]**
200	410	65	6.3
250	560	85	6.6
300	670	105	6.4
350	810	122	6.6
400	760	120	6.3
450	870	138	6.3
500	840	133	6.3

Table 11 Results from experiment with straight blades

Figure 47 shows the development of the car alternator rotational speed in relation to the volume flow rate. The x-axis represents the volume flow rate in $[l\ s^{-1}]$ from $200l\ s^{-1}$ to $500l\ s^{-1}$ and on the y-axis the rotational speed of the car alternator in $[min^{-1}]$ can be seen. The graph depicts an increase in rotational speed at the beginning and a stagnation in the end. The rotational speed of the car alternator increases with a raising volume flow rate in the water channel from $200l\ s^{-1}$ to $350l\ s^{-1}$. Afterwards the rotational speed starts to stagnate from $350l\ s^{-1}$ to $500l\ s^{-1}$. At a volume flow rate of approximately $350l\ s^{-1}$ and $450l\ s^{-1}$a slight decrease in rotational speed can be observed. The figure indicates that, even if a raise in volume flow rate should lead to an increase in the rotational speed of the car alternator, the rotational speed starts to stagnate starting from a volume flow rate of around $350l\ s^{-1}$.

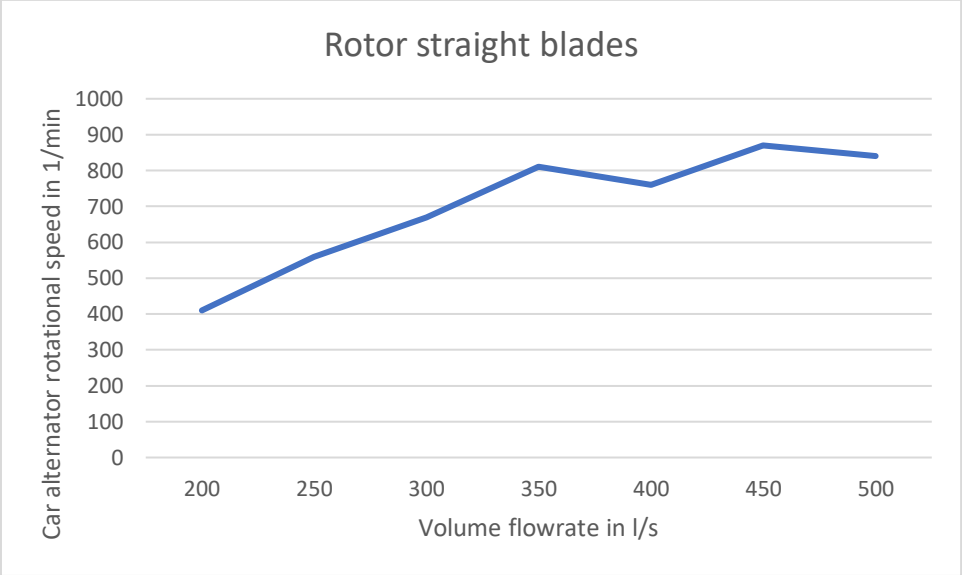

Figure 47 Development of car alternator rotational speed for rotor with straight blades

8.2.4 Results straight blades

The experiment has been repeated with the same volume flow rate for the second rotor design with rounded blades. Table 12 represents the results of the test with rounded blades. Also, the second experiment with a different rotor geometry proposed an increase of rotational speed at the beginning and a stagnation of rotational speed at a further raise in volume flow rate. Nevertheless, the rotational speed of the car alternator was increasing from $200l\ s^{-1}$ to $250l\ s^{-1}$ and started already to stagnate from $300l\ s^{-1}$ to $500l\ s^{-1}$. Even if the second rotor design achieved higher rotational speeds from $200l\ s^{-1}$ to $300l\ s^{-1}$, the rotational speed attained at volume flowrates between $300l\ s^{-1}$ to $500l\ s^{-1}$ were close to the rotational speeds from the test of the rotor with straight blades. The experiment also showed that due to friction losses a drop in the transmission ratio from the ideal value of 6.7 to around 6.3 occurred. Also, the second rotor construction did not achieve the desired rotational speed of the car alternator of approximately $1600min^{-1}$.

Volume flow rate supplied by pump [$\frac{l}{s}$]	Alternator rotational speed [$\frac{1}{min}$]	Rotor rotational speed [$\frac{1}{min}$]	Transmission Ratio [-]
200	490	75	6.5
250	630	100	6.3
300	740	120	6.2
350	770	125	6.2
400	840	133	6.3
450	810	126	6.4
500	840	133	6.3

Table 12 Results from experiment with rounded blades

Figure 48 shows the development of the car alternator rotational speed in relation to the volume flow rate for the rotor with rounded blades. The x-axis resembles the volume flow rate applied in the water channel in $[l\ s^{-1}]$ and the y-axis shows the rotational speed of the car alternator in $[min^{-1}]$. The graph represents an increase in rotational speed at low volume flow rates and a stagnation for large volume flow rates. From $200l\ s^{-1}$ to $350l\ s^{-1}$ the rotational speed of the car alternator increases at a constant rate. Afterwards a stagnation of the rotational speed takes part between the values of $350l\ s^{-1}$ to $500l\ s^{-1}$. The figure shows that even in the second experiment with a different rotor geometry the rotational speed of the car alternator increases at the beginning with a raising volume flowrate but starts to stagnate after a volume flow rate of approximately $300l\ s^{-1}$.

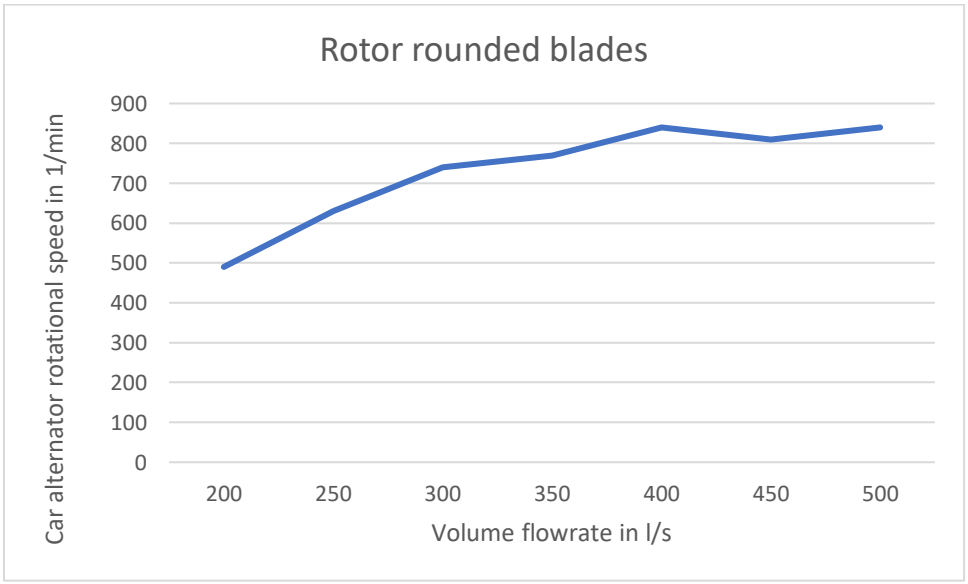

Figure 48 Development of car alternator rotational speed for rotor with rounded blades

8.2.5 Comparison rotor with straight blades and rotor with rounded blades

Figure 49 compares the development of the car alternator rotational speed attained from the rotor with straight blades and the rotor with rounded blades. The x-axis resembles the volume flow rate in $[l\ s^{-1}]$ from $200l\ s^{-1}$ to $500l\ s^{-1}$ and the y-axis shows the rotational speed of the car alternator in $[min^{-1}]$. The graph shows that the rotational speed of both rotor designs increases at the beginning but starts to stagnate in the end. Furthermore, the graph depicts that the rotor with rounded blades outputs a higher rotational speed than the rotor with straight blades at the beginning but starts to align with the values of the rotor with straight blades at higher volume flow rates. Till around $300l\ s^{-1}$ the rotor with rounded blades lead to a rotational speed, which is approximately $60min^{-1}$ to $70min^{-1}$ higher than the rotor design with straight blades. Nevertheless, the rotational speeds start to align with their values exceeding a volume flow rate of approximately $300l\ s^{-1}$.The rotor with rounded blades even reaches slightly lower values at $350l\ s^{-1}$ and $450l\ s^{-1}$. The figure shows that the rotor with rounded blades leads to a higher rotational speed at low volume flowrates, nevertheless this trend does not proceed and after around $300l\ s^{-1}$ the attained rotational speeds start to equalize.

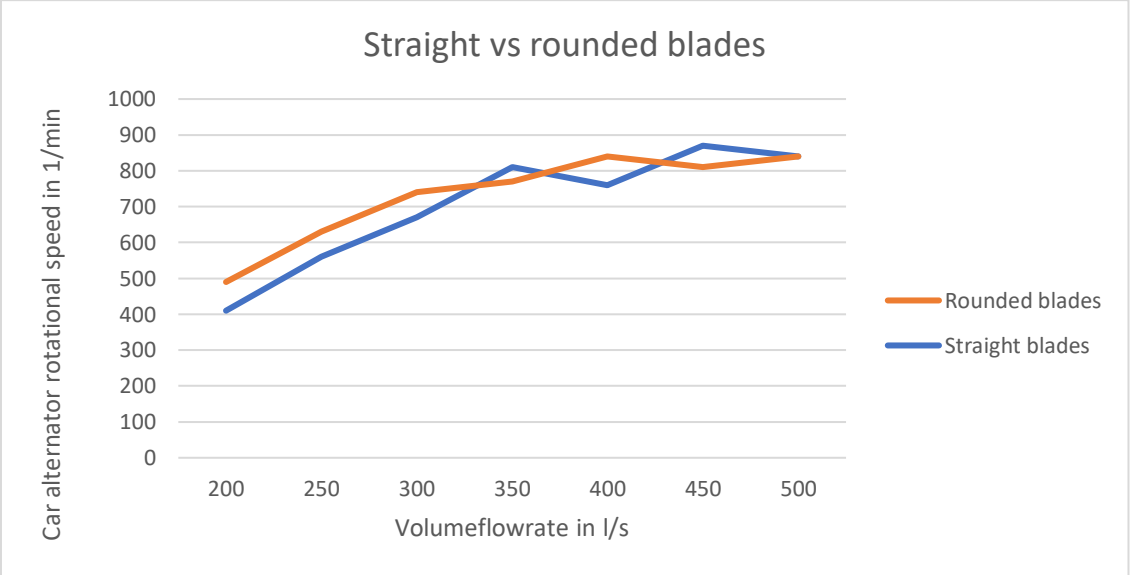

Figure 49 Comparison rotational speed rotor with straight and with rounded blades

8.2.6 Results

After having analyzed the outcomes and the results from the experiments the following potential improvements have been discussed. The rotational speed of the rotor has been successfully transmitted to the car alternator. Nevertheless, due to slip conditions between the inner tube, the rotor and the car alternator, the desired transmission ratio of around 6.7 has not been achieved. The transmission ratios resulting from the experiments (see table 11 and 12) lie between 6.2 and 6.5. Therefore, the transmission ratio should still be optimized and further suitable materials for the transmission should be tested.

Furthermore, the experiments showed that the theoretical rotational speed of the car alternator of approximately $1600\ min^{-1}$ at a speed in the water channel of around $0.5m\ s^{-1}$ has not been achieved. The rotational speed of the car alternator at a flow rate of $0.5m\ s^{-1}$ in the water channel resulted in $840\ min^{-1}$(see table 11 and 12) for the rounded and the straight blades. One reason for the deviation in the desired and obtained rotational speed and for the stagnation after a certain volume flow rate in the channel may be that a certain part of the volume flows aside the vortex flow turbine, as the sides are not dammed. This may cause a stagnation of the volume flow rate flowing inside the vortex flow turbine and results in a stagnation of the rotational speed. Therefore, a test has been performed (see section 8.3) where the open spots between the vortex flow turbine and the water channel have been blocked to prevent that the water can flow aside the turbine.

To increase the transmission between the rotor and the car alternator, a motorcycle rim with a bigger diameter could be chosen. Due to time reasons the rim will not be replaced, but in section 9.2.5 the advantages will be discussed as a potential improvement for the future.

A further option to attain the desired power output would be to adjust the car alternator. By rewinding the car alternator, the needed rotational speed to attain a certain voltage output can be adjusted. Therefore, the number of windings can be reduced to achieve a voltage output at around $840\ min^{-1}$. The process of rewinding a car alternator is sophisticated and time consuming and lies therefore out of the scope of this project. Nevertheless, the process and potential advantages of rewinding the car alternator will be described in section 9.2.6 as a potential improvement worth considering in the future.

8.3 Blocking the sides of the channel

The test performed in section 8.2 proposed that the rotational speed of the rotor and the car alternator start to stagnate at a volume flowrate of around $300\ l\ s^{-1}$ to $350\ l\ s^{-1}$. This result is unexpected as an increase in volume flow rate should lead to an increase of the rotational speed. A possible reason for this effect may be that the open spots between the vortex flow turbine and the water channel have not been dammed (see figure 50) and most of the volume flow rate just flowed aside the turbine and the volume flow rate passing the turbine started to stagnate.

Due to the stagnation of the rotational speed, which may be caused due to the water flowing rather aside the turbine then inside the turbine, the open spots between the vortex flow turbine and the water channel have been blocked (see figure 50). Furthermore, a blockage of the water also allows to simulate more realistic testing results as the vortex will not be generated anymore due to a pressure difference, but due to a difference in height. Additionally, the moment of the rotor will be measured to calculate the power at the shaft of the vortex flow turbine.

The target of the test is to attain more realistic test results, which coincide more with results under vortex turbine design conditions and to perform a test with an elimination of volume flow rate losses aside the open spots between the vortex flow turbine and the water channel.

Figure 50 Experimental set-up with blocked sides

8.3.1 Testing procedure

The vortex flow turbine can be put in the water channel with the help of straps and can be fixed by placing stones on the wooden pallet (see figure 50). However, this time the open spots between the vortex flow turbine and the water channel will be closed with wooden pallets and steel plates (see figure 50). Nevertheless, apart from the blockage aside the turbine, the test will be not performed with the same volume flow rates as in the experiment in section 8.2. The volume flow rate in the channel will be slowly increased till the maximum value where the water in the channel does just not flood the turbine and will afterwards be constantly operated under this volume flow rate.

Then with an oscilloscope the rotational speed of the rotor and the car alternator will be measured and documented. The target is to attain results, which coincide more with the operation of the vortex flow turbine under vortex turbine design conditions. In this experiment the moment of the rotor will also be measured with the help of a spring scale. The spring scale will be fixed on the motorcycle rim during the operation of the vortex flow turbine and the applied force by the rotor then can be measured. To attain the moment under which the turbine operates, the distance between the point where the spring scale has been fixed to and the axis of the rotor shaft can be measured. By multiplying the previously measured force with the distance between spring scale and rotor axis, the moment can be calculated. With the rotational speed of the rotor and the moment, the power at the turbine shaft can be calculated (see formulas below). The abbreviations of the formulas can be seen in the nomenclature in section 13.

The experiment will be performed twice, once for the rotor with straight blades and once for the rotor with rounded blades. This test should deliver more accurate results, as the testing conditions are closer to the vortex flow design conditions.

Moment

$$M = F \cdot d$$

Angular velocity

$$\omega = 2 \cdot \pi \cdot N$$

Power at the turbine shaft

$$P_{shaft\ turbine} = M \cdot \omega$$

8.3.2 Performed experiments

The volume flow rate has been increased slowly till the maximum volume flow rate has been achieved before the turbine will be flooded. The maximum achieved volume flow rate in the water channel has been approximately $125\ l\ s^{-1}$. Also, in this experiment a proper vortex has been induced inside the oil barrel. Nevertheless, in this test the vortex has been induced due to the height difference between inlet and outlet and not because of the creation of an under pressure with a gate at the outlet's opening. As the area of the water channel is approximately $1m^2$ and the channel has been dammed, the flow rate inside the channel started to strive towards zero. Nevertheless, the testing conditions lead to more realistic results as a height difference between inlet and outlet has been simulated.

The experiment has been performed twice. One time for the rotor with straight blades and once again for the rotor with rounded blades. The results of both tests can be seen in table 13. The highest rotational speed achieved in the experiment in section 8.2.3 and 8.2.4 has been around $840\ min^{-1}$ for both rotor designs. In the experiment with blocked sides the rotational speed attained for the rotor with straight blades has been approximately $890\ min^{-1}$ and around $920\ min^{-1}$ for the rotor design with rounded blades. The rotational speed attained for the rotor with straight blades has been around $138\ min^{-1}$ and $146\ min^{-1}$ for the rotor with rounded blades. This resulted in similar transmission ratios of 6.3 for the rotor with rounded blades and 6.5 for the rotor with straight blades. The force applied to the spring scale has been around 35N for both rotor geometries, which leads, by a lever arm of around 0.17m, to a moment of 6Nm (See calculations below). The abbreviations of the formulas can be seen in the nomenclature in section 13. The detailed calculation of the hydraulic power for both rotor designs can be seen below and leads to a power at the turbine shaft of around 86.7W for the rotor with straight blades and to 91.7W for the rotor with rounded blades.

Calculation for rotor with straight blades:

$$M = F \cdot d = 35N \cdot 0.17m = 6Nm$$

$$\omega_{straight\ blades} = 2 \cdot \pi \cdot N_{straight\ blades} = 2 \cdot \pi \cdot 138min^{-1} = 867.08min^{-1} \triangleq 14.45s^{-1}$$

$$P_{shaft\ turbine,\ \ straight\ blades} = M \cdot \omega_{straight\ blades} = 6Nm \cdot 14.45s^{-1} = 86.7W$$

Calculation for rotor with rounded blades:

$$M = F \cdot d = 35N \cdot 0.17m = 6Nm$$

$$\omega_{rounded\ blades} = 2 \cdot \pi \cdot N_{rounded\ blades} = 2 \cdot \pi \cdot 146min^{-1} = 917.35min^{-1} \triangleq 15.29s^{-1}$$

$$P_{shaft\ turbine,rounded\ blades} = M \cdot \omega_{rounded\ blades} = 6Nm \cdot 15.29s^{-1} = 91.7W$$

	Volume flow rate supplied by pump $[\frac{l}{s}]$	Alternator rotational speed $[\frac{1}{min}]$	Rotor rotational speed $[\frac{1}{min}]$	Transmission Ratio [-]	Force [N]	Lever arm [m]	Moment [Nm]	Shaft turbine power [W]
Straight blades	125	890	138	6.5	35	0.17	6	86.7
Rounded blades	125	920	146	6.3	35	0.17	6	91.7

Table 13 Experimental results with blocked sides

8.3.3 Results

The hydraulic power of the vortex flow turbine lies in the range of around 90W, which provides a first impression at which range of performance the vortex flow turbine can be operated. The rotational speed for both rotor geometries have been higher compared to the rotational speeds from the experiment in section 8.2. This results as the vortex has be produced due to the height difference between inlet and outlet and not due to a creation of under pressure.

Nevertheless, the desired flow rate of around $0.5m\ s^{-1}$ in the water channel has not been able to generate. Therefore, it can be expected that by adjusting the experiment to a set-up which coincides even more with the vortex flow design conditions, a higher rotational speed should be attained. Under real operations at a river, a side channel would have to be created. To conduct such an experiment a channel with the same dimensions as the inlet opening must be constructed, which would allow a higher water speed entering the vortex flow turbine. A possible set up of the adjustment of the experiment can be seen in figure 51.

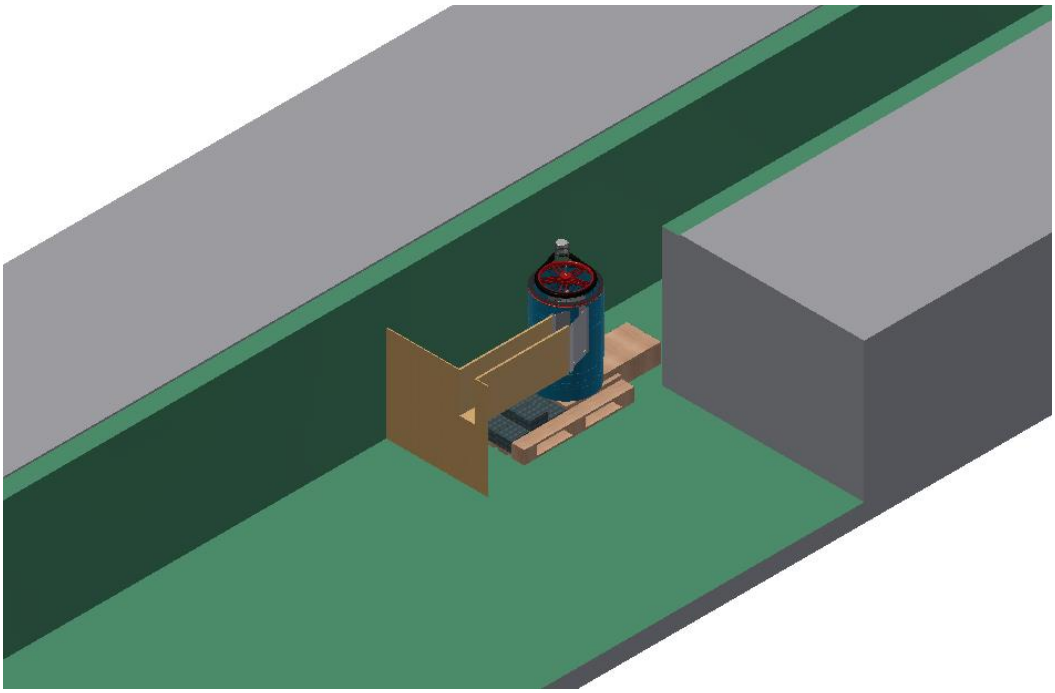

Figure 51 Theoretical set-up with wooden channel added

8.4 Testing the car alternator

The testing of the car alternator aims to attain the behavior of the voltage, the current and the moment at rotational speeds up to $1600\ min^{-1}$ under different loads. Moreover, the characteristic curve of the car alternator under no-load condition and the minimum voltage, which must be delivered by the battery to induce a magnetic field in the inner coil of the car alternator will be measured.

The type of car alternator used for the experiment has the engine description “TypA127IR-85A”. As the car alternator used in the test has a coil fixed on its rotor instead of a permanent magnet, a battery has been needed to induce a magnetic field in the inner coil. The car alternator tested can be seen in figure 52.

In the previous industrial project (Ritz, 2020) the car alternator was not tested, but experimental results from the Lancaster university were obtained and used as reference values. They attained at a rotational speed of around $1600\ min^{-1}$ a voltage output of approximately 12V and a current of 2A under no-load conditions. Nevertheless, in the scope of this project a car alternator will be tested in the HSLU laboratory to gain a better understanding of the behavior of the car alternator at different rotational speeds.

Figure 52 Car alternator used for the testing's

8.4.1 Testing procedure

The test fixture is a metal plate with boreholes and a motor fixed to it. The car alternator can be fixed to the metal plate with two angel irons as it can be seen in figure 53. The car alternator then can be coupled to the motor with a claw coupling. To fix the counter part of the claw coupling to the car alternator, the claw coupling must be adjusted with two threaded holes and a hull must be manufactured to adjust the diameter of the threaded axis of the car alternator. The hull can be clamped with a nut to the threaded axis of the car alternator and the claw coupling can be fixed afterwards to the hull with two grub screws.

If the testing fixture is prepared, the experiment to produce the voltage, current and moment of the car alternator at different loads can be performed. For this test, the rotational speed of the motor must be increased in steps of $100\ min^{-1}$ from $100\ min^{-1}$ to $1600\ min^{-1}$. It is recommended to perform the test with different loads to understand how the characteristic curve of the voltage and the current are influenced by the magnitude of the load. In the scope of this experiment two different loads have been tested at 60W and 100W.

The second experiment, which will be performed is the testing of the car alternator with no load applied to the car alternator to attain the characteristic curve of the car alternator under no-load

conditions. The rotational speed will also be increased in steps of $100\ min^{-1}$ from $100\ min^{-1}$ to $1600\ min^{-1}$. The target is to obtain the characteristic curve of the voltage output in relation to the rotational speed applied to the car alternator. By attaining the characteristic curve of the car alternator, it can be seen at which rotational speeds the car alternator has to be operated to produce a certain voltage output.

The third experiment discusses the question of the minimum voltage, which is required to induce a magnetic field in the inner coil of car alternator. The battery will be connected to the car alternator and voltages from 1V to 14V in steps of 1V will be applied to the inner coil. The rotor then will be operated under a rotational speed of around $1100\ min^{-1}$ and afterwards the voltage generated by the car alternator under a battery voltage from 1V to 14V can be measured. It can then be observed, which is the minimum voltage that must be delivered by the battery so that the car alternator generates a voltage output.

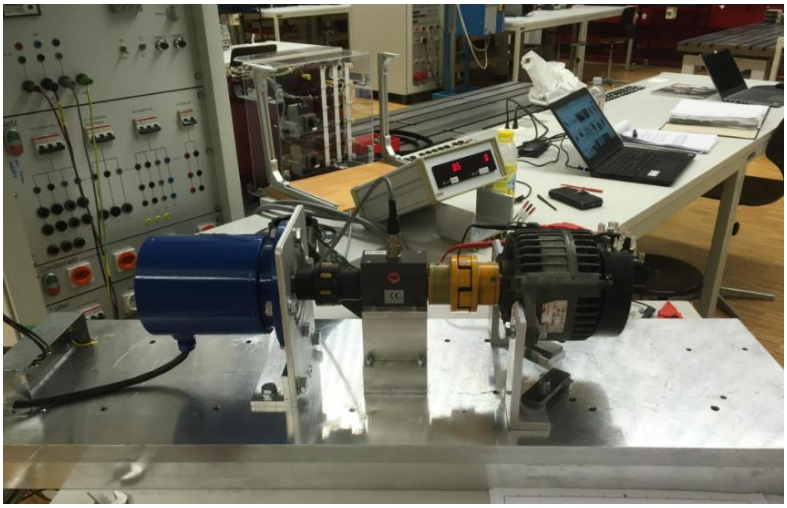

Figure 53 Experimental set-up to test car alternator

8.4.2 Performed experiments

After the car alternator has been installed on the testing fixture and the battery for the bias voltage has been loaded, the three tests have been performed and the experimental results have been analyzed.

In the first experiment the car alternator has been tested for loads of 60W and 100W. To induce a magnetic field in the inner coil of the car alternator, a battery has been loaded to a bias voltage of around 13V. Afterwards the rotational speed applied to the car alternator has been increased from $100\ min^{-1}$ to $1600\ min^{-1}$ in steps of $100\ min^{-1}$. The produced voltage, current and moment at the different rotational speeds have been noted and listed in a table (see section 8.4.3 and section 8.4.4). The results of the performed experiment for 60W can be seen in section 8.4.3 and for a load of 100W in section 8.4.4.

In the second experiment the characteristic curve of the car alternator under no-load condition has been created. To create the characteristic curve, also a battery with a bias voltage has been connected to the car alternator. The rotational speed was afterwards raised from $100\ min^{-1}$ to $1600\ min^{-1}$. In the test with no load applied to the car alternator, only the voltage output has been measured (see section 8.4.5). The obtained characteristic curve can be seen on page 51.

In the third experiment the minimum voltage to induce a magnetic field in the inner coil of the car alternator has been measured. The battery has been loaded to around 14V and has been discharged continuously in steps of 1V to the final value of 1V. The car alternator has been driven by a motor and the voltage output at different voltages provided by the battery have been measured. The results of the experiment can be seen in section 8.4.6.

8.4.3 Results for a 60W load

The first experiment has been performed under a load of approximately 60W. The starting voltage of the battery, before connecting it to the car alternator, was 12.895V. With these settings the car alternator has been tested for rotational speeds from $100\ min^{-1}$ to $1600\ min^{-1}$. The results of the experiment can be seen in table 14.

The voltage of the battery started to decrease between the rotational speeds of $100\ min^{-1}$ and $900\ min^{-1}$ (see table 14). This drop in voltage implies that by applying a rotational speed below $900\ min^{-1}$ to the car alternator, the battery is being discharged instead of charged. This is because the voltage needed to induce a magnetic field in the inner coil, a higher voltage supply is needed than the car alternator generates under operation with rotational speeds below $900\ min^{-1}$. Nevertheless, from $900\ min^{-1}$ to $1600\ min^{-1}$ the voltage starts to increase. Therefore, it can be concluded that if the car alternator is operated at a rotational speed above $900\ min^{-1}$, the car alternator generates a higher voltage output than is used for the generation of the magnetic field in the inner coil. Furthermore, the table shows that the current drops when the voltage increases, so that the power output of the car alternator is always around 60W. The moment increases from a rotational speed of $100\ min^{-1}$ to $1200\ min^{-1}$ and then starts to decrease from a rotational speed of $1200\ min^{-1}$ to $1600\ min^{-1}$. The reason for the drop in moment after a rotational speed of $1200\ min^{-1}$ may be that the car alternator starts to be operated closer to its ideal operation point.

The figure 54 on page 47 provides a better understanding of the behavior of the voltage and the current and depicts the tipping point of the rotational speed above which the car alternator should be operated.

Rotational speed $\left[\frac{1}{min}\right]$	**Voltage** $[V]$	**Current** $[A]$	**Electric power** $[W]$	**Moment** $[Nm]$	**Power Load [W]**
100	12.2	4.9	59.78	0.5	60
200	12.15	4.93	59.8995	0.5	60
300	12.12	4.94	59.8728	0.5	60
400	12.11	4.95	59.9445	0.5	60
500	11.75	5.1	59.925	1.1	60
600	11.73	5.11	59.9403	1.1	60
700	11.74	5.1	59.874	1.1	60
800	11.73	5.11	59.9403	1.2	60
900	11.74	5.11	59.9914	1.2	60
1000	12.06	4.97	59.9382	1.6	60
1100	12.65	4,74	59.961	2.5	60
1200	13.32	4.5	59.94	3.3	60
1300	13.49	4.44	59.8956	3.1	60
1400	13.56	4.42	59.9352	2.7	60
1500	13.6	4.41	59.976	2.4	60
1600	13.62	4.4	59.928	2.3	60

Table 14 Experimental results for a load of 60W

Figure 54 shows the development of the voltage and the current in comparison to the rotational speed applied to the car alternator. The x-axis depicts the rotational speed of the car alternator from $100\ min^{-1}$ to $1600\ min^{-1}$. The y-axis resembles on the left y-axis the voltage output in $[V]$ from the car alternator and on the right side the current in $[A]$ attained from the car alternator. The graph shows that the voltage decreases from $100\ min^{-1}$ to $500\ min^{-1}$. From $500\ min^{-1}$ to $900\ min^{-1}$ the voltage stays constant at around 11.75V. At a rotational speed of approximately $900\ min^{-1}$, the voltage output from the car alternator starts to increase sharply till around $1200\ min^{-1}$ where the increase in voltage starts to flatten out. The tipping point of the car alternator lies at a rotational speed of approximately $900\ min^{-1}$. The graph shows that if the car alternator is operated at a rotational speed below $900\ min^{-1}$, the car alternator consumes more voltage from the battery than it generates. If the car alternator exceeds the rotational speed of around $900\ min^{-1}$ the car alternator produces more voltage than the battery delivers.

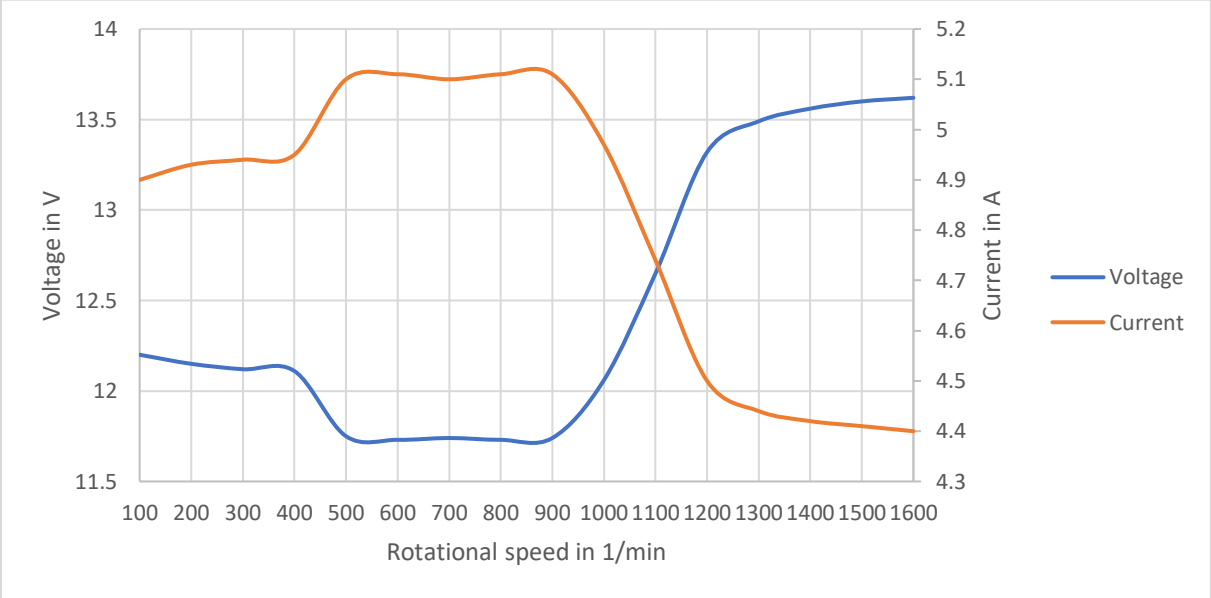

Figure 54 Graph behavior voltage and current for a load of 60W

8.4.4 Results for a 100W load

In the last test the load has been increased to 100W. The bias voltage of the battery, before having been attached to the car alternator, has been 13.078V. The rotational speed of the car alternator has been increased from $100\ min^{-1}$ to $1600\ min^{-1}$ in steps of $100\ min^{-1}$.

The table shows that the voltage in the battery decreased between the rotational speeds of $100\ min^{-1}$ to $900\ min^{-1}$. This drop in voltage implies that the car alternator consumes more voltage than it generates in the range of $100\ min^{-1}$ to $900\ min^{-1}$. From a rotational speed of $900\ min^{-1}$ to $1600\ min^{-1}$ the voltage starts to increase. This increase in voltage shows that above $900\ min^{-1}$ the car alternator generates more voltage than the battery must deliver to induce the magnetic field in the coil. The table proposes that if the voltage increases the current drops and if the voltage decreases the current increases. This relationship leads to a constant output of 100W and is reached due to the control unit in the car alternator. The moment increases from a rotational speed of $100\ min^{-1}$ to $1300\ min^{-1}$ and starts to decrease after exceeding the rotational speed of $1300\ min^{-1}$. This drop in moment follows the same pattern as in the experiment with 60W in section 8.4.3 and may also be caused since the car alternator starts to be operated closer to its ideal operation point.

The figure 56 on page 49 shows the relationship of the voltage and the current to the rotational speed of the car alternator in more detail. Furthermore, the tipping point above which the car alternator should be operated can be observed.

Rotational speed $\left[\frac{1}{min}\right]$	**Voltage** $[V]$	**Current** $[A]$	**Electric power** $[W]$	**Moment** $[Nm]$	**Power Belastung [W]**
100	11.908	8.377	99.753316	0.6	100
200	11.911	8.39	99.93329	0.6	100
300	11.9	8.4	99.96	0.6	100
400	11.89	8.4	99.876	0.5	100
500	11.61	8.6	99.846	1	100
600	11.606	8.61	99.92766	1.1	100
700	11.65	8.58	99.957	1.1	100
800	11.65	8.582	99.9803	1.2	100
900	11.65	8.57	99.8405	1.2	100
1000	11.91	8.39	99.9249	1.6	100
1100	12.43	8.03	99.8129	2.5	100
1200	12.96	7.71	99.9216	3.3	100
1300	13.3	7.52	100.016	3.4	100
1400	13.35	7.48	99.858	3	100
1500	13.4	7.46	99.964	2.8	100
1600	13.42	7.45	99.979	2.7	100

Figure 55 Experimental results for a load of 100W

Figure 56 illustrates the relationship of the voltage and the current in comparison to the rotational speed of the car alternator. The x-axis shows the rotational speed of the car alternator ranging from $100\ min^{-1}$ to $1600\ min^{-1}$. The y-axis depicts two y-axes, on the left side the voltage in $[V]$ and on the right side the current in $[A]$. From $500\ min^{-1}$ to $900\ min^{-1}$ the voltage stays constant and starts to increase after around $900\ min^{-1}$. Above a rotational speed of $900\ min^{-1}$, the voltage output from the car alternator increases drastically up to a rotational speed of around $1300\ min^{-1}$. After a rotational speed of around $1300\ min^{-1}$ the voltage still increases, but at a lower rate than between $900\ min^{-1}$ to $1300\ min^{-1}$. The graph indicates that by operating the car alternator at a rotational speed below $900\ min^{-1}$ more voltage is consumed by the car alternator from the battery than is delivered from the car alternator to the battery. If the car alternator is operated at a rotational speed above $900\ min^{-1}$ the car alternator delivers more voltage to the battery than the car alternators consumes from the battery.

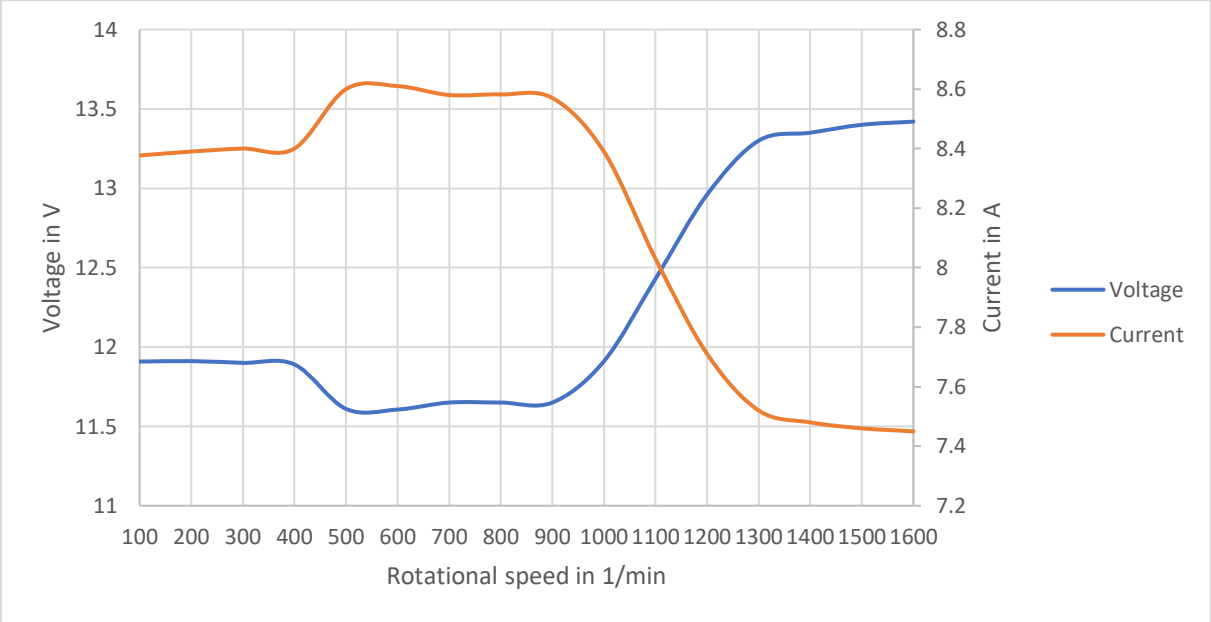

Figure 56 Graph behavior voltage and current for a load of 100W

8.4.5 Characteristic curve under no-load condition

To obtain the characteristic curve of the car alternator, the car alternator has been operated under rotational speeds from $100\ min^{-1}$ to $1600\ min^{-1}$ with no load applied to the car alternator. Afterwards the voltage output for the different rotational speeds has been measured. The starting voltage of the battery was around 12.815V.

By testing the car alternator under no-load conditions, the characteristic curve of the car alternator can be determined and a detailed overview of the behavior of the voltage generation of the device can be created. The experiment showed that the voltage of the battery drops till around $900\ min^{-1}$ and then starts to increase again after exceeding a rotational speed of around $900\ min^{-1}$. Therefore, under no-load conditions the car alternator starts to generate an excess voltage only after approximately $900\ min^{-1}$. It can be observed that the behavior of the voltage in relation to the rotational speed did not deviate significantly from the results obtained from the experiments in section 8.4.3 and section 8.4.4 with a load of 60W and 100W applied to the car alternator. The moment and the current output have not been measured, as only the voltage output was of significant interested in the plotting of the characteristic curve.

To understand the development of the voltage over the different rotational speeds, the characteristic curve on page 51 can be analyzed. The characteristic curve of the car alternator under no-load conditions supports the understanding of the voltage development inside the car alternator.

Rotational speed $\left[\frac{1}{min}\right]$	**Voltage** $[V]$
100	12.808
200	12.806
300	12.804
400	12.804
500	12.45
600	12.39
700	12.42
800	12.41
900	12.41
1000	12.61
1100	13.08
1200	13.39
1300	13.46
1400	13.5
1500	13.53
1600	13.55

Figure 57 Voltage attained at different rotational speeds under no-load condition

The figure 58 depicts the characteristic curve of the car alternator under no-load conditions. On the x-axis the rotational speed of the car alternator from $100\ min^{-1}$ to $1600\ min^{-1}$ is displayed in increasing steps of $100\ min^{-1}$. The y-axis shows the voltage in the battery in $[V]$. The figure indicates that the voltage stays constant from a rotational speed of $100\ min^{-1}$ to $400\ min^{-1}$. After exceeding $400\ min^{-1}$ the voltage in the battery drops from around 12.8V to approximately 12.4 and remains at that voltage till $900\ min^{-1}$. If the car alternator exceeds a rotational speed of $900\ min^{-1}$ the voltage in the battery starts to increase sharply till around $1200\ min^{-1}$ and still increases from $1200\ min^{-1}$ to $1600\ min^{-1}$, but at a lower rate than from $900\ min^{-1}$ to $1200\ min^{-1}$. The graph shows the characteristic behavior of the voltage generation of the car alternator in relation to the rotational speed applied. Furthermore, the figure points out that the car alternator must exceed a rotational speed of around $900\ min^{-1}$ to generate an excess voltage.

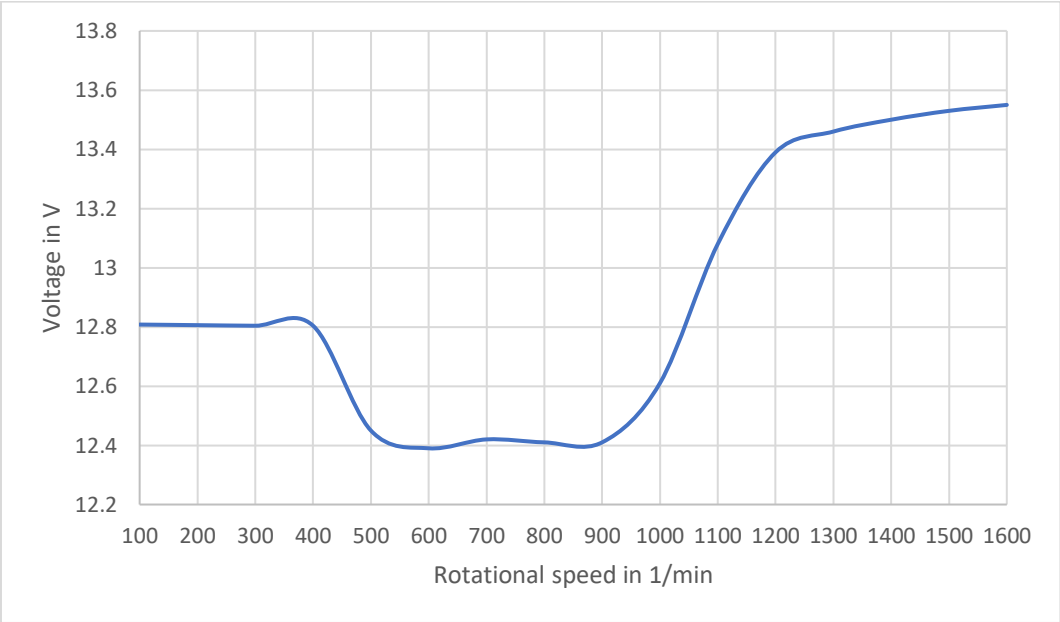

Figure 58 Characteristic curve of the car alternator

8.4.6 Test of minimum voltage needed from battery

To determine the minimum voltage needed from the battery to allow an induction of the inner coil, the car alternator has been tested for different battery voltages (see table 15 left column). Furthermore, the voltage generated by the car alternator at the specific voltages of battery have been measured accordingly (see table 15 right column).

The experiment showed that the minimum voltage which must be delivered by the battery is at least 5V. At approximately 5V the car alternator generates a voltage of approximately 12.46V. Furthermore, the test showed that from 5V to 13V the car alternator produces a stable voltage output, which stays in the range of 12.46V to 12.62V. Nevertheless, if the voltage of the battery is between 1V to 4V, the car alternator is not able to generate any voltage as the delivered voltage of the battery is not high enough to induce a magnetic field inside the inner coil. Therefore, it can be concluded that the bias voltage, which must be delivered by the battery to the car alternator must be at least 5V.

Nevertheless, it should be considered that the battery used to provide the bias voltage to the car alternator should not be discharged below the recommended off-load-voltage of the battery. For instance, it is proposed that a car battery should not be discharged below 12.3V (So zerstörst Du Deine Autobatterie! I Wie geht man mit Batterien um? I Tutorial I ARS24, 2015). If a car battery is discharged below the off-load-voltage, the battery can be damaged and its expected lifetime will decrease. The reason is that by undercutting the off-load-voltage, the electrolyte in the battery is not equally distributed over the lead plate, which may prevent that the energy can be received properly. Therefore, even if a voltage of around 5V is enough to induce a magnetic field in the inner coil of the car alternator, it is not recommended to discharge a battery below its off-load-voltage.

Voltage delivered by the battery $[V]$	**Voltage generated by the car alternator $[V]$**
13	12.62
12	12.58
11	12.47
10	12.46
9	12.46
8	12.46
7	12.46
6	12.46
5	12.46
4	0
3	0
2	0
1	0

Table 15 Voltage generate at different bias voltages

8.5 Experiment with wooden channel in front

The experiment in section 8.3 with blocked sides of the vortex flow turbine did not coincide with the vortex turbine design conditions, as the water entered the vortex flow turbine with a too low flow rate. To achieve the flow rate of around $0.5m\ s^{-1}$,for which the vortex flow turbine has been calculated in the industrial project (Ritz, 2020), a wooden channel has been crafted and connected to the inlet of the turbine (see figure 59). The channel had the same dimensions as the inlet of the vortex flow turbine and had the target to increase the velocity with which the water enters the turbine.

By increasing the flow rate of the water in the wooden channel to approximately $0.5m\ s^{-1}$, the rotational speed of the rotor and the car alternator can be measured under a more realistic operation set-up, which allows a better understanding of the potential performance of the vortex flow turbine. Therefore, it can be measured if the car alternator is able to excess the rotational speed of around $900\ min^{-1}$ to generate an excess voltage under no-load conditions.

Furthermore, the hydraulic power, the power at the shaft and the efficiency will be calculated. With the formula $P_{hydraulic} = Q \cdot H \cdot \rho \cdot g$ the hydraulic power of the turbine can be calculated. The volume flow rate Q can be attained by measuring the velocity in the wooden channel and multiplying it with the area of the wooden channel. Afterwards, the power on the shaft can be calculated by multiplying the moment applied to the rotor with the angular velocity. The efficiency then can be calculated by dividing the power at the shaft by the hydraulic power of the turbine. The formulas can be seen below, and the nomenclature can be found in section 13.

Hydraulic power

$$\frac{p_1}{\rho} + g \cdot h_1 + \frac{{v_1}^2}{2} = \frac{p_2}{\rho} + g \cdot h_2 + \frac{{v_2}^2}{2} + g \cdot H$$

with $p_1 = p_2 = p_{atmosphere}$

$$g \cdot h_1 + \frac{{v_1}^2}{2} = g \cdot h_2 + \frac{{v_2}^2}{2} + g \cdot H$$

Due to visual observations during the test, it can be assumed that $v_1 \approx v_2$

$$g \cdot h_1 - g \cdot h_2 = g \cdot H$$

$$H = h_1 - h_2$$

$$P_{hydraulic} = Q \cdot H \cdot \rho \cdot g$$

Power at the turbine shaft

$$M = F \cdot d$$

$$\omega = 2 \cdot \pi \cdot N$$

$$P_{shaft\ turbine} = M \cdot \omega$$

Efficiency

$$\eta = \frac{P_{shaft\ turbine}}{P_{hydraulic}}$$

8.5.1 Testing procedure

To increase the flow rate of the water entering the vortex flow turbine, a wooden channel with the dimensions $190mm \cdot 430mm$ must be created and connected to the inlet of the turbine. To stabilize the wooden channel, a wooden beam construction which connects the water channel and the wooden channel can be manufactured. Furthermore, to connect the wooden channel with the inlet of the vortex flow turbine duct tape is recommended to be used. Duct tape allows a simple and impermeable connection of the two components. The constructed wooden channel can be seen in figure 59.

The experiment will be performed for both rotor geometries to allow a comparison of the performance of both rotor designs. Furthermore, the test is aimed to reach a flow rate in the wooden channel as close as possible to $0.5m\ s^{-1}$. The test targets to measure the volume flow rate in the wooden channel, the moment of the rotor and the rotational speed of the car alternator and the rotor. To attain the volume flow rate inside the wooden channel, the flow rate and the area of the channel must be measured. The flow rate can be measured by placing a wooden piece inside the wooden channel and counting the time the wooden piece needs to cover a certain distance. The distance, which was covered by the wooden piece at a certain time can be simply measured with a ruler. By multiplying the flowrate and the area of the wooden channel, the volume flow rate inside the wooden channel can be obtained. The moment of the rotor can be measured by applying a spring scale on the motorcycle rim and multiplying the attained force with the distance from the spring scale to the axis of the rotor. The rotational speed of the car alternator and the rotor can be measured with an oscilloscope. The experimental results and measured values out of the test can be seen in section 8.5.2.

Figure 59 Experimental set-up with added wooden channel

8.5.2 Performed experiments

After having constructed the wooden channel and having connected the wooden channel to the vortex flow turbine, the water channel has been filled with water. The volume flow rate delivered by the pump has been increased till the maximum, just before the vortex flow turbine has been flooded. Furthermore, the height difference between the inlet and outlet of the turbine has been measured to be around $0.85m$. The experiment has been performed for both rotor designs to see the difference of rotational speed for the different rotors.

In the first experiment the rotor with straight blades has been tested. By applying a feather scale at the motorcycle rim at a distance of $0.17m$ to the axis of the rotor, a force of $33N$ has been measured. By multiplying the distance with the force, it can be calculated that the rotor operates under a moment of approximately $5.6Nm$. Afterwards the rotational speed of the car alternator and the rotor has been measured with an oscilloscope and resulted in $145min^{-1}$ for the rotor and in $948min^{-1}$ for the car alternator. To measure the flow rate in the wooden channel, a wooden piece has been put into channel and the time the wooden piece needed for covering $1m$ has been timed. By multiplying the velocity with the area of the wooden channel, the volume flow rate inside the wooden channel has been determined to be around $0.032m^3s^{-1}$.

Having performed the test for the rotor with straight blades, the experiment with the same set-up has been repeated for the rotor geometry with rounded blades. The feather scale has also been applied to approximately $0.17m$ and a force of $40N$ has been measured. This resulted in a moment at the rotor of around $6.8Nm$. With the oscilloscope the rotational speed at the car alternator and the rotor has been measured and a rotational speed of $146min^{-1}$ for the rotor and a rotational speed of $954min^{-1}$ for the car alternator has been measured. The volume flow rate has also been measured by counting the time a wooden piece needs to cover $1m$. By multiplying the flow rate in the wooden channel with its area, it was calculated that the volume flow rate in the wooden channel is around $0.032m^3s^{-1}$. The experimental data attained from the test can be seen in the table 16 below.

	Speed in the wooden channel [$\frac{m}{s}$]	**Alternator rotational speed [$\frac{1}{min}$]**	**Rotor rotational speed [$\frac{1}{min}$]**	**Transmission Ratio [-]**	**Force [N]**	**Lever arm [m]**	**Moment [Nm]**	**Area of water channel [m^2]**	**Volume flow rate in wooden channel [$\frac{m^3}{s}$]**
Rotor with straight blades	0.4	948	145	6.5	33	0.17	5.6	0.08	0.032
Rotor with rounded blades	0.4	954	146	6.5	40	0.17	6.8	0.08	0.032

Table 16 Experimental results for vortex flow turbine with added wooden channel

8.5.3 Results

After having performed the experiment and measured the rotational speeds, the moments and the volume flow rate in the wooden channel, the hydraulic power, the power at the rotor shaft and the efficiency of the vortex flow turbine can be calculated for both rotor geometries. Furthermore, the attained rotational speed at the car alternator can be compared with the needed rotational speed tested for the car alternator under no-load conditions in section 8.4.5. The calculations for both rotor designs can be seen below and the nomenclature can be found in section 13.

The hydraulic power of the turbine is for both rotor geometries around 266.83W. By multiplying the moment at the car alternator with the angular velocity at the rotor, it can be calculated that the power at the shaft is for the rotor with straight blades approximately 85W and for the rotor with rounded blades around 103.97W. By dividing the power of the shaft by the hydraulic power it can be observed that the vortex flow turbine reaches an overall efficiency for the rotor with straight blades of 31.86% and for the rotor with rounded blades of around 38.97%. Therefore, it can be concluded that for the rotor with rounded blades a 7% higher efficiency can be reached. Nevertheless, as the difference in efficiency is only around 7%, it is also worth considering installing the rotor with straight blades as its construction is simpler and less time consuming.

The rotational speed attained for both rotor geometries is around $950 min^{-1}$ (see table 16 in section 8.5.2). It should be considered that the car alternator has been tested under no-load conditions. Therefore, the car alternator has been operated under no internal resistance, as the magnetic field in the inner coil of the car alternator has not been induced with a bias voltage. Nevertheless, a first insight can be attained of the rotational speed, which can be achieved with the vortex flow turbine under no-load conditions. By comparing the attained rotational speed of the vortex flow turbine and the required rotational speed to generate an excess voltage from the experiment in section 8.4.5, it can be concluded that the car alternator exceeds the $900 min^{-1}$ and would lie in the range of generating an excess voltage. It is still worth considering optimizing the vortex flow turbine to reach a higher rotational speed to exceed the rotational speed of $900 min^{-1}$ even more and test the vortex flow turbine with a magnetic field induced in the car alternator to attain results with a resistance.

Rotor with straight blades

$$P_{hydraulic} = Q \cdot h \cdot \rho \cdot g = 0.032 m^3 s^{-1} \cdot 0.85 m \cdot 1000 kg\ m^{-3} \cdot 9.81 m\ s^{-2} = 266.83 W$$

$$M = F \cdot d = 33 N \cdot 0.17 m = 5.6 Nm$$
$$\omega = 2 \cdot \pi \cdot N = 2 \cdot \pi \cdot 145 min^{-1} = 911.06 min^{-1} \triangleq 15.18 s^{-1}$$
$$P_{shaft\ turbine} = 5.6 Nm \cdot 15.18 s^{-1} = 85 W$$

$$\eta = \frac{P_{shaft\ turbine}}{P_{hydraulic}} = \frac{85W}{266.83W} = 0.32 \triangleq 31.86\%$$

Rotor with rounded blades

$$P_{hydraulic} = Q \cdot h \cdot \rho \cdot g = 0.032 m^3 s^{-1} \cdot 0.85 m \cdot 1000 kg\ m^{-3} \cdot 9.81 m\ s^{-2} = 266.83 W$$

$$M = F \cdot d = 40 N \cdot 0.17 m = 6.8 Nm$$
$$\omega = 2 \cdot \pi \cdot N = 2 \cdot \pi \cdot 146 min^{-1} = 917.35 min^{-1} \triangleq 15.29 s^{-1}$$
$$P_{shaft\ turbine} = 6.8 Nm \cdot 15.29 s^{-1} = 103.97 W$$

$$\eta = \frac{P_{shaft\ turbine}}{P_{hydraulic}} = \frac{103.97W}{266.83W} = 0.39 \triangleq 38.97\%$$

9. Improvement of the vortex flow turbine

The design of the vortex flow turbine has been adjusted regarding the developed vortex flow turbine in the industrial project (Ritz, 2020). The final construction and design of the vortex flow turbine faced certain optimizations regarding its functionality and feasibility.

The first sub section “9.1 Improvements during construction” discusses improvements of the vortex flow turbine design, which have been performed during the construction of the vortex flow turbine. Whereas the second sub section “9.2 Potential future improvements” shows improvements and optimizations, which could be potentially made in the future.

9.1 Improvements during construction

During the construction process of the vortex flow turbine certain improvements regarding the design of the turbine have been performed. The physical construction of the vortex flow turbine provided an insight into certain construction challenges and design flaws, which had to be optimized.

The following section discusses the design improvements, which have been performed during the construction of the vortex flow turbine from the industrial project (Ritz, 2020) to the current vortex flow turbine design. The figures 60 and 61 below show the differences of the 3D-model from the industrial project and the bachelor thesis.

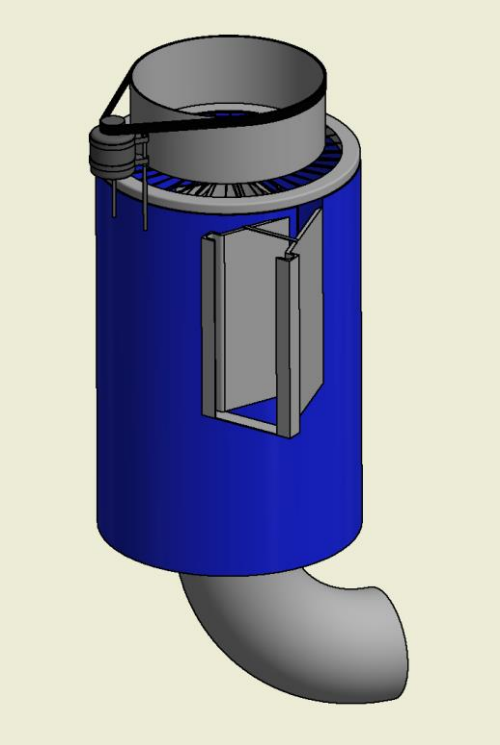

Figure 60 Developed vortex flow turbine in industrial project

Figure 61 Optimized vortex flow turbine bachelor thesis

9.1.1 Outlet became made of wood

One element which faced a change in its design, during the construction process, was the outlet of the vortex flow turbine. The design of the outlet was changed from consisting of an elbow pipe (see figure 62) with a diameter of 254mm to a squarish wooden channel (see figure 63).

One reason for the replacement of the pipe elbow by a wooden channel was the acquisition process of the pipe elbow, which showed that finding a pipe elbow with a specific diameter is not a simple process. Wooden plates on the other hand are much more likely to be attained and therefore simplify the acquisition process.

Furthermore, during the construction process the problem occurred that it is not feasible to weld the elbow pipe to the oil barrel, as the wall thickness of the pipe elbow and the oil barrel are deviating too much. Therefore, a sophisticated construction would have been required to be developed to connect the pipe elbow to the oil barrel, whereas the wooden shaft construction can simply be screwed to the oil barrel.

The pipe elbow is heavier in its weight compared to the wooden channel. By replacing the pipe elbow by the wooden channel, the overall weight of the vortex flow turbine can be reduced and simplifies the transportation of the vortex flow turbine from the place of construction to the river.

Figure 62 Elbow pipe as outlet

Figure 63 Wooden channel as outlet

9.1.2 Fixation of the vortex flow turbine

In the industrial project (Ritz, 2020) the fixation of the vortex flow turbine and the detailed operated conditions have not been discussed. Therefore, a method for the fixation of the vortex flow turbine to its surroundings has been proposed.

A wooden pallet has been fixed to the oil barrel to provide the vortex flow turbine with a stable basis (see figure 64). The vortex flow turbine can be fixed in the channel by putting stones on the empty place of the wooden pallet. The number of stones depends on the river conditions and must be chosen such as the turbine is not flushed away by the river stream.

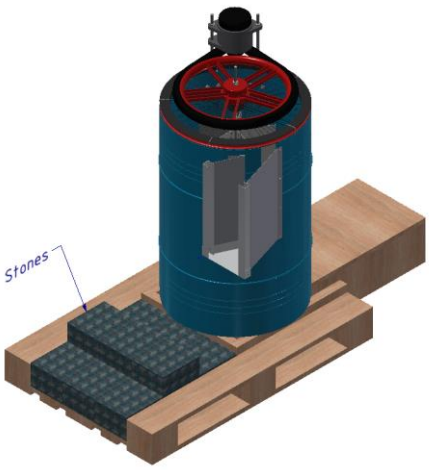

Figure 64 Vortex flow turbines with stones for fixation

9.1.3 Sheet metal instead of welded inlet

A further improvement which has been made during the manufacturing process of the vortex flow turbine was an adjustment of the construction of the inlet.

In the industrial project (Ritz, 2020) the inlet was proposed to be manufactured as a welded construction. Nevertheless, constructing the inlet in form of a sheet metal, instead of a welded construction, allows a simpler construction process by not requiring welding equipment. Once the sheet metal is drawn on an aluminum plate, the tools needed for the manufacturing of the inlet are a hammer, a saw and a drill. Furthermore, if the inlet is constructed as a sheet metal, aluminum can be used as the material and reduces the weight of the inlet. A reduced weight of the inlet construction allows a simpler transportation of the vortex flow turbine and simplifies its connection to the oil barrel. Considering the advantage of a more rudimentary construction and the reduction in weight, the inlet was redesigned from a welded construction to a sheet metal construction (see figure 65 and figure 66).

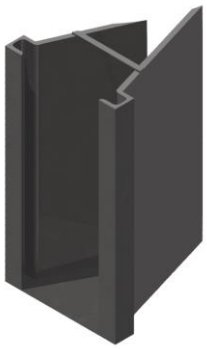

Figure 65 Inlet developed in industrial project

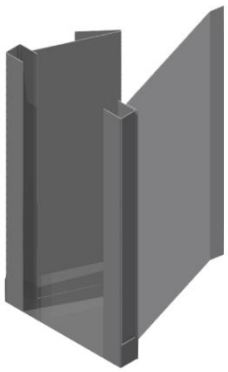

Figure 66 Optimized inlet bachelor thesis

9.1.4 Motorcycle rim instead of car rim

During the acquisition process of the scrap parts for the vortex flow turbine, the realization came that the weight of a car rim made of steel has been underestimated in the industrial project (Ritz, 2020). Therefore, the question was raised if there may be a lighter substitute for the car rim, which constitutes of approximately the same diameter.

As a potential alternative a motorcycle rim made of aluminum has been proposed. The substitution of the car rim with a motorcycle rim resulted in a weight reduction of the transmission of approximately 6-7 kilogram. This saving in weight allowed the turbine to be operated at a lower turning moment and increased the turbines overall efficiency. Furthermore, the constant strain the transmission applies on the bearing has been reduced and results in a higher life expectancy of the bearing of the vortex flow turbine.

Also, the construction effort was reduced by replacing the car rim with a motorcycle rim. In the industrial project (Ritz, 2020) the connection of the car rim to the shaft was planned with a sophisticated welding connection. The motorcycle rim on the other hand allowed a rudimentary connection to the rotor shaft with a clamping connection with 4 nuts. In figure 67 and 68 the impact of the change from the car rim to the motorcycle rim can be seen and it can be observed that figure 68 resembles a lighter and less bulky design than the construction in figure 67.

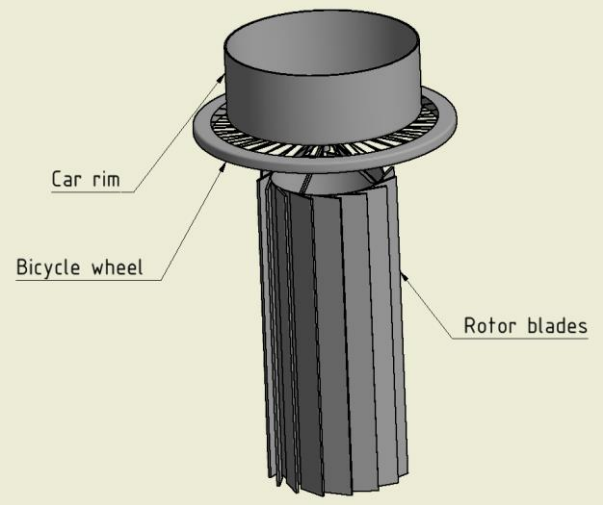

Figure 67 Rotor developed in industrial project

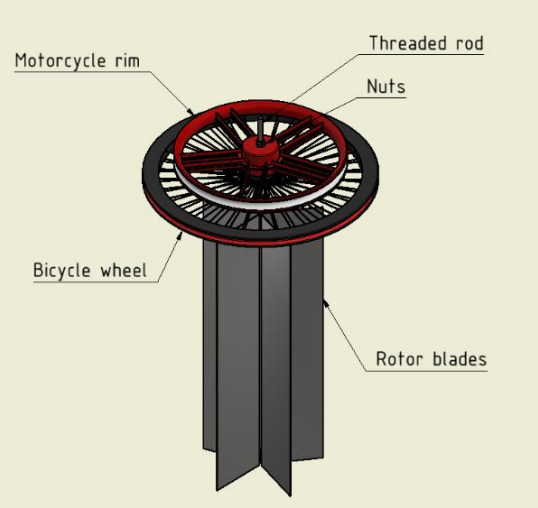

Figure 68 Optimized rotor

9.1.5 Transmission

In the industrial project (Ritz, 2020) the application of a connection of two v-belts for the transmission of the turning moment from the rotor to the car alternator was planned. Nevertheless, the connection of two v-belts, to attain the desired distance between rotor and car alternator, was practically not feasible and a new alternative for the transmission had to be developed. Furthermore, the acquisition process of the scrap parts declared that searching for a v-belt with the exact diameter required is not realistic and is very unlikely to be found on a scrap yard.

In the scope of the project suitable scrap parts for the transmission have been searched and tested. The test has been of rudimentary manner. The potential transmission parts have been installed on the vortex flow turbine and the motorcycle rim has been rotated manually with approximately one rotation per minute. This test delivered quick results if a scrap part is suitable and transmits the moment properly. Three scrap parts have been tested such as a connection of tights (see figure 69), a rubber rope (see figure 70) and the inner tube of a 16-inch motorcycle rim (see figure 71).

The tights transmitted the moment from the motorcycle rim to the car alternator properly, nevertheless the transmission resulted in a low transmission ratio as the slip effect was severe. Therefore, the tights have been considered as not suitable as the slip losses do not allow an efficient exploitation of the rotational speed.

The testing of the rubber rope showed that the friction area of the rubber rope is not big enough to allow a proper transmission of the rotational speed. Furthermore, the rubber rope solved itself from the freewheel of the car alternator during the manual rotation of the motorcycle rim. Therefore, also the rubber rope did not fulfill the properties to transmit the rotational speed from the motorcycle rim to the car alternator properly.

As the last part the inner tube of the 16-inch motorcycle rim (see figure 71) has been tested. The inner tube can be stretched to the diameter needed and transmits the rotational moment actuated by coherence. Furthermore, the inner tube can be easily acquired as the part is usually attached to the motorcycle rim, which also is required for the development of the vortex flow turbine. Therefore, the inner tube of the motorcycle rim has been determined to be the most suitable scrap part for the transmission of the scrap part materials collected and tested.

Figure 69 Tights

Figure 70 Rubber rope

Figure 71 Inner tube

9.2 Potential future improvements

Apart from improvements which have been performed during the construction process of the vortex flow turbine, the bachelor thesis also proposes optimizations, which can be undertaken in the future or during a reconstruction of the developed vortex flow turbine. This section discusses improvements, which may be worth to consider if the vortex flow turbine is planned to be improved.

9.2.1 Bucket as possible protection

A potential source of danger which may damage the car alternator are high tidal waves, which may flood the car alternator. To prevent a potential destruction of the car alternator, a sealing consisting of a plastic bucket has been proposed. Nevertheless, the necessity of such a covering of the car alternator depends on the river conditions.

The construction of the covering can simply be constructed by machining a plastic bucket (see figure 72). A plastic bucket is a scrap part, which can be found easily and does not underlie any dimension requirements, if it covers the car alternator fully and protects the device from a potential intrusion of water. Nevertheless, the slot for the transmission should be construction big enough to prevent friction losses between the plastic bucket and the inner tube.

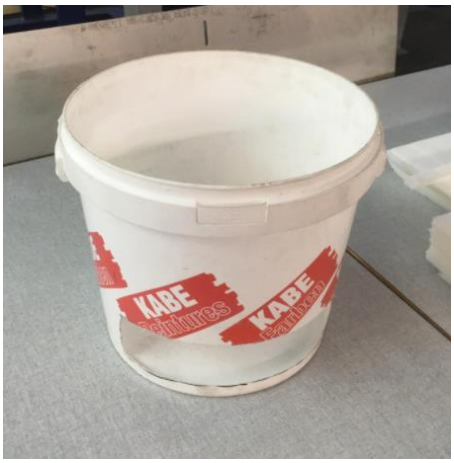

Figure 72 Plastic bucket

9.2.2 Better material for the transmission

The testing of the vortex flow turbine in section 8.5 showed that there is slip due to friction losses between the inner tube and the car alternator. The ideal transmission ratio would be around 6.7, whereas the actual attained transmission ratio lies in the range of 6.3 to 6.5. The section “Transmission” on page 61 discusses the materials, which have already been consider aside of the inner tube of a motorcycle and the reasons why they have not been considered as suitable.

In the scope of this project no material for the transmission has been found, which would lead to a more efficient transmission. Nevertheless, this does not imply that there are no scrap parts, which may lead to a better transmission then the inner tube of a motorcycle rim.

Therefore, it is proposed to search for further suitable transmission materials, as a more efficient transmission would directly lead to a higher rotational speed of the car alternator.

9.2.3 Testing under real operation conditions

The testing of the vortex flow turbine in the water channel of the HSLU laboratory showed that the vortex flow turbine cannot be operated by being installed directly in an open river. It is recommended to create a side channel next to the river were the vortex flow turbine can be installed (see figure 73). This section proposes a suitable construction of the side channel of the vortex flow turbine under vortex turbine design conditions.

In the first steps a side channel must be dug next to a river. The channel leading the water flow into the vortex flow turbine should have the same dimensions as the inlet of the turbine. Whereas the channel connected to the outlet of the vortex flow turbine should have the same width as the oil barrel. After having dug the side channel, the vortex flow turbine can be placed in the channel and fixed by putting stones on the wooden pallet. Afterwards the empty spots at the inlet side can be covered with soil to allow a straight water flow into the inlet (see figure 73).

The flow rate entering the vortex flow turbine should lie in the range of approximately $0.5m\ s^{-1}$. A simple way to measure the flow rate in the soil channel before the turbines inlet is by placing a piece of wood or plastic into the channel and measure the time the part needs for traveling 1m. The particle should approximately need around 2 seconds to travel the distance of 1m. If more accuracy is need, the same procedure can be repeated for 5m, which should be achieved in around 10 seconds. To adjust the flow rate in the soil channel, the entrance of the channel can be dammed with stones.

By operating the vortex flow turbine under the described conditions, the height difference between inlet and outlet can be exploited in the most efficient set-up and an optimal rotational speed of the rotor and the car alternator can be obtained.

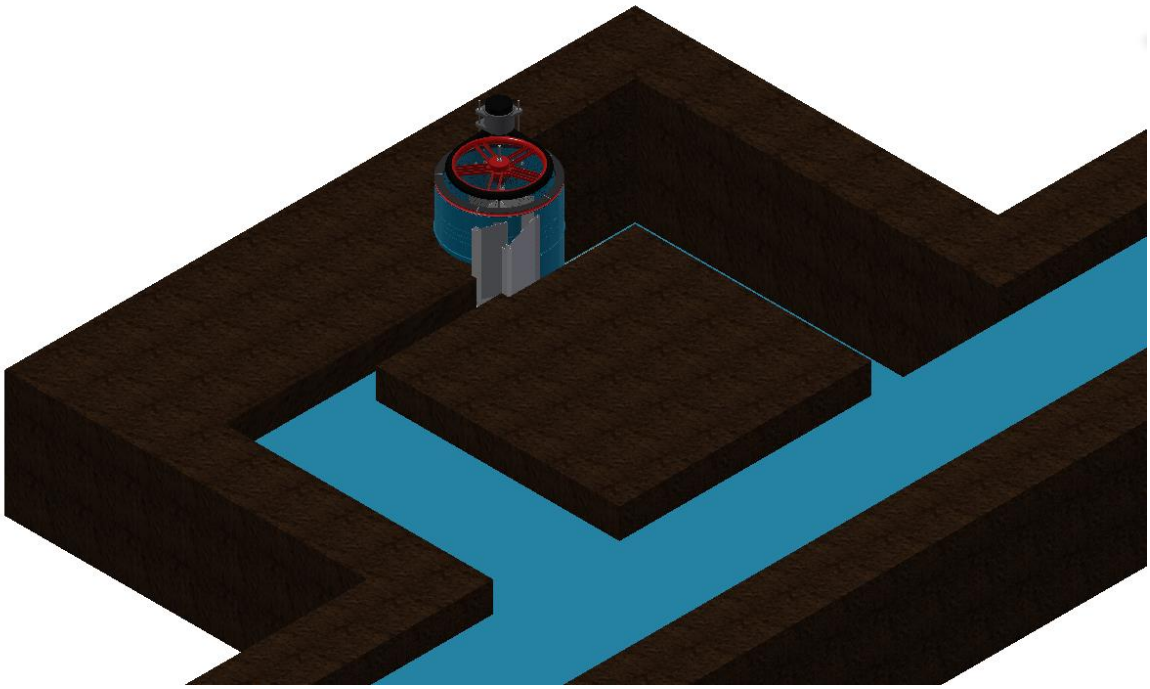

Figure 73 Installation of vortex flow turbine under real operation conditions

9.2.4 Sealing with cloth parts

During the construction process of the bachelor thesis a lot of welded construction parts have been replaced by screwed constructions. This replacement leads to a simplification in the overall construction process and skill needed for the construction of the vortex flow turbine, but also leads to a worse sealed construction unit.

Therefore, during the testing phase of the vortex flow turbine the idea has been raised to seal the parts, which were screwed. The sealing can be achieved by cutting old cloths or towels into strips and clamp them between the two parts, which must be screwed together. Using cloths or towels as a sealing, the impermeability of the overall turbine can be increased significantly. In the figure 74 strips cut out from an old towel can be seen, which have been used for the sealing of the inlet. Other parts of the vortex flow turbine such as the outlet are suggested to be also sealed with old cloth parts or towels.

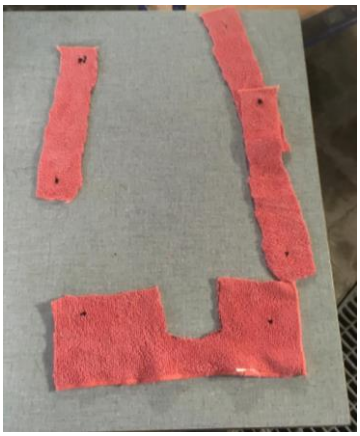

Figure 74 Towels used for sealing

9.2.5 Test with a 17-inch motorcycle rim

A further improvement for future optimization processes of the vortex flow turbine could be the replacement of the 16-inch motorcycle rim with a 17-inch motorcycle rim. An increase in diameter of the motorcycle rim would also lead to an increase in transmission ratio and this would result in a higher rotational speed at the car alternator. Nevertheless, by replacing the 16-inch motorcycle rim with a 17-inch motorcycle rim, the distance of the car alternator to the rim must be increased accordingly to avoid a collision of the two components.

The theoretical achievable transmission ratio could be increased from around 6.7 to 7.1. The diameter of the alternator freewheel was measured to be approximately 61mm. The calculation of the transmission ratio of the 16-inch and the 17-inch motorcycle rim can be seen below.

Calculation for 16-inch motorcycle rim (16-inch≙406,4mm):

$$Transmission\ ratio = \frac{motorcycle\ rim\ diameter}{alternator\ freewheel\ diameter} = \frac{406{,}4mm}{61mm} = 6.7$$

Calculation for 17-inch motorcycle rim (17-inch≙431,8mm):

$$Transmission\ ratio = \frac{motorcycle\ rim\ diameter}{alternator\ freewheel\ diameter} = \frac{431.8mm}{61mm} = 7.1$$

9.2.6 Rewinding the car alternator

The tests performed in the thesis showed that the rotational speed achieved by the car alternator laid in the range of around $950min^{-1}$. As car alternators are usually laid-out for higher rotational speeds, an adjustment of the car alternator has been considered. This section discusses an adjustment of the number of windings of a car alternator to reduce the rotational speed required for a voltage output of around 12V.

The paper (Carrillo, 2012) examines the influence of an increase in windings on the rotational speed required to reach a voltage output of approximately 12V. In the first part of the paper the number of windings to achieve a voltage output of around 12V have been calculated. Afterwards the car alternator has been rewound with the number of windings calculated. In the next step, the rewound car alternator has been tested and the voltage output has been measured. A Toyota car alternator has been used for the rewinding and the testing.

They recalculated the number of windings to attain a voltage output of 12V for a rotational speed of the car alternator of approximately $200min^{-1}$. The calculation yielded in 376 windings, which resulted in 63 turns à 6 bundles. As the area did not provide the surface capacity for 63 turns, the turns have been reduced to 40 windings, which resulted in 240windings. The inner part of the rewound car alternator can be seen in figure 75.

The test of the rewound car alternator yielded to the following conclusion. The voltage output of around 12V cannot be achieved at around $200min^{-1}$, nevertheless the 12V can be achieved at approximately $800min^{-1}$. This leads to the conclusion that by rewinding the car alternator, the required rotational speed to output 12V can be reduced to $800min^{-1}$ and would fall into the rotational speed range attained from the vortex flow turbine developed and tested in this project. As the rewinding process of a car alternator is not of a rudimentary manner and requires a certain time investment, a repetition of the experiment has been excluded of the thesis. Nevertheless, for future improvements of the vortex flow turbine the option of rewinding the car alternator can still be considered.

Figure 75 Rewound car alternator

9.2.7 Testing of the car alternator not under no-load conditions

In the scope of this project, the vortex flow turbine has been tested under no-load conditions of the car alternator. This means that no bias voltage has been applied to the car alternator to generate a magnetic field inside the car alternator. If a bias voltage will be delivered to the inner coil of the car alternator, a magnetic field will be induced, which leads to a resistance in the car alternator. Due to time reasons no electrical set-up was constructed to provide the car alternator with a bias voltage and a load to test the car alternator. Therefore, the overall vortex flow turbine has only been tested under no-load conditions. It is recommended for future improvements of the vortex flow turbine to perform an experiment with a load applied to the car alternator.

A similar set-up as in the experiment in section 8.4 (see figure 76 below) can be arranged in the HSLU laboratory next to the vortex flow turbine. Afterwards a bias voltage from a battery can be delivered to the car alternator to generate a magnet field in the inner coil of the car alternator, which leads by operation of the vortex flow turbine to an inner resistance of the car alternator. The electrical control unit should be designed in a way that different loads such as for instance 60W or 100W can be tested such as in the experiment in section 8.4. By inducing a magnetic field in the inner coil of the car alternator, the rotational speed of the car alternator and the rotor can be determined with an inner resistance of the car alternator. This adjustment of the experiment would lead to results, which are closer to the real operation of the vortex flow turbine. Furthermore, it can be measured if an excess voltage in the car alternator can be achieved, while the car alternator is loaded with an inner resistance. The experimental set-up also allows to attain an insight into how much the rotational speed is affected by the inner resistance of the car alternator and if the transmission must be further optimized due to additional slip.

Figure 76 Control unit used to test car alternator

10. Conclusion

In the scope of this project a vortex flow turbine, which is applicable for developing countries has been constructed out of scrap parts. Afterwards the vortex flow turbine has been tested in the water channel in the HSLU laboratory to examine the achievable performance of the turbine.

The construction of the vortex flow turbine was successful and even optimizations and improvements were performed during the construction process of the turbine. Furthermore, the achievable rotational speeds of the rotor and the car alternator of the vortex flow turbine have been tested under no-load conditions. The outcome was that the generator can be operated under a rotational speed of approximately $950 min^{-1}$ and the rotor under around $145 min^{-1}$. The car alternator has also been tested to generate its characteristic curve and understand its behavior. The main outcome was that the car alternator must be operated at a rotational speed of at least $900 min^{-1}$ to generate an excess voltage. Nevertheless, the vortex flow turbine has only been tested under no-load conditions and the experimental set-up did not exactly coincide with the vortex turbine design conditions.

The work provided an insight in a first testing of the vortex flow turbine and examined which possible performance and rotational speeds can be achieved. The thesis delivered a good basis for further improvements of the vortex flow turbine and discussed further optimizations. Furthermore, the thesis delivers a constructed vortex flow turbine, which provides an understanding of the function and potential of a rudimentary vortex flow turbine, which leads to a ground base for further optimization processes to reach an ideal outcome.

It is recommended to test the vortex flow turbine also with an inner resistance applied to the car alternator to also attain test results, which have not been tested under no-load conditions. This would lead to even more realistic testing results and a more accurate understanding of the performance of the vortex flow turbine can be gathered. Also, the outcome of the thesis suggests to further optimize the geometry and the design of the rotor and to test the vortex flow turbine in a more real-world applied set-up.

11. Figures

Unless stated in parentheses, all figures are own creations.

12. Tables

13. Nomenclature

Symbol	Description	SI-Unit
Q	Volume flow rate	$\left[\frac{m^3}{s}\right]$
P_e	Electrical power	$[W]$
$P_{shaft\ turbine}$	Power at turbine shaft	$[W]$
$P_{hydraulic}$	Hydraulic power	$[W]$
H	Water head	$[m]$
ρ	Density	$\left[\frac{kg}{m^3}\right]$
g	Gravity	$\left[\frac{m}{s^2}\right]$
N	Revolution	$\left[\frac{1}{s}\right]$
η	Efficiency	$[-]$
U	Voltage	$[V]$
I	Current	$[A]$
M	Moment	$[Nm]$
F	Force	$[N]$
d	Distance	$[m]$
ω	Angular speed	$\left[\frac{1}{s}\right]$
F	Force	$[N]$
d	Distance	$[m]$
p_1	Pressure at inlet	$[Pa]$
p_2	Pressure at outlet	$[Pa]$
$p_{atmosphere}$	Pressure at atmosphere	$[Pa]$
h_1	Height at inlet	$[m]$
h_2	Height at outlet	$[m]$
v_1	Velocity at inlet	$\left[\frac{m}{s}\right]$
v_2	Velocity at outlet	$\left[\frac{m}{s}\right]$

14. List of references

Ritz, J. (2020). Development of a vortex flow turbine for developing countries. Switzerland: Horw

Carrillo, Y. (2012) Retrofitting a Car Alternator for Low-Speed Power Generation. California

Pongaskorn, W. & Ratchapon, S. (2016) The Effects of Turbine Baffle Plates on the Efficiency of Water Free Vortex Turbines. Japan: Kitakyushu

Sitriam, P. & Suntivarakom R. (2019) The effects of blade number and turbine baffle plates on the efficiency of free-vortex water turbines. Thailand: Khon Kaen

Youtube. (2015, November 27). So zerstörst Du Deine Autobatterie! I Wie geht man mit Batterien um? I Tutorial I ARS24. Retrieved from: https://www.youtube.com/watch?v=O4bLmVz9CLU

Laden einer Batterie. (n.d.). Retrieved from: https://www.varta-automotive.ch/de-ch/varta-batteriewissen/laden/laden-einer-autobattrie

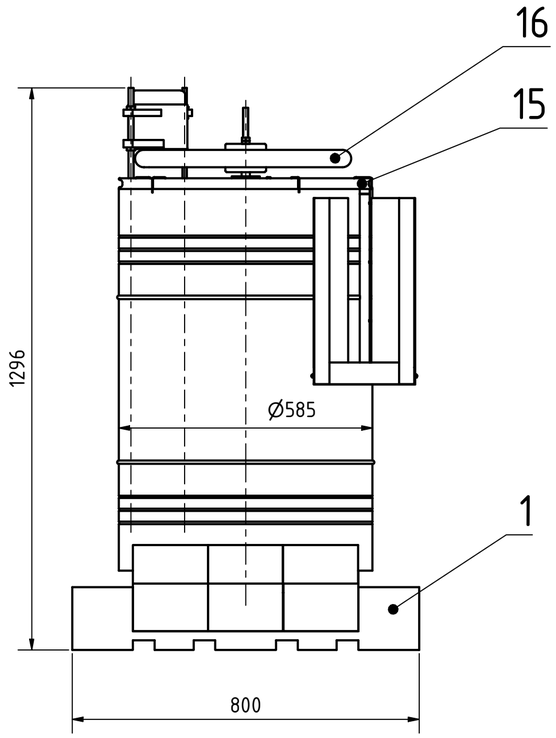

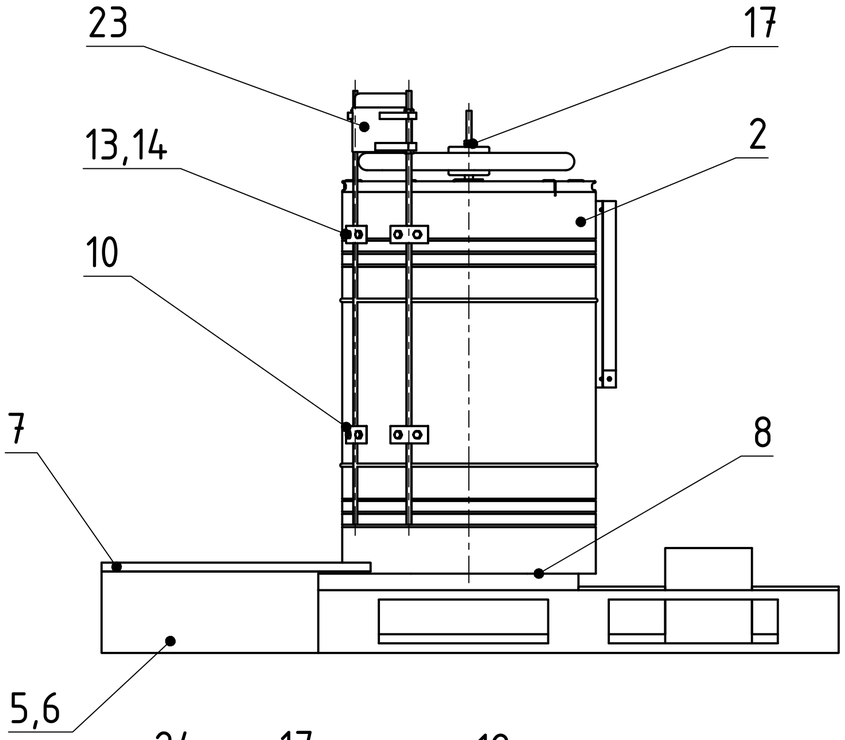

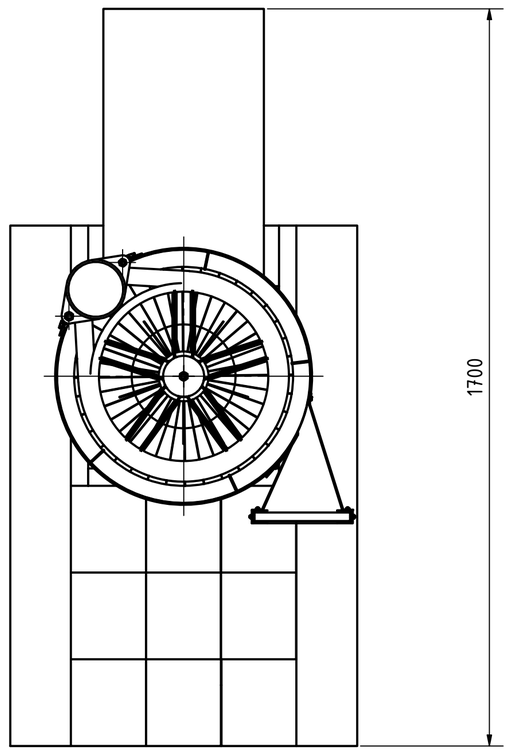

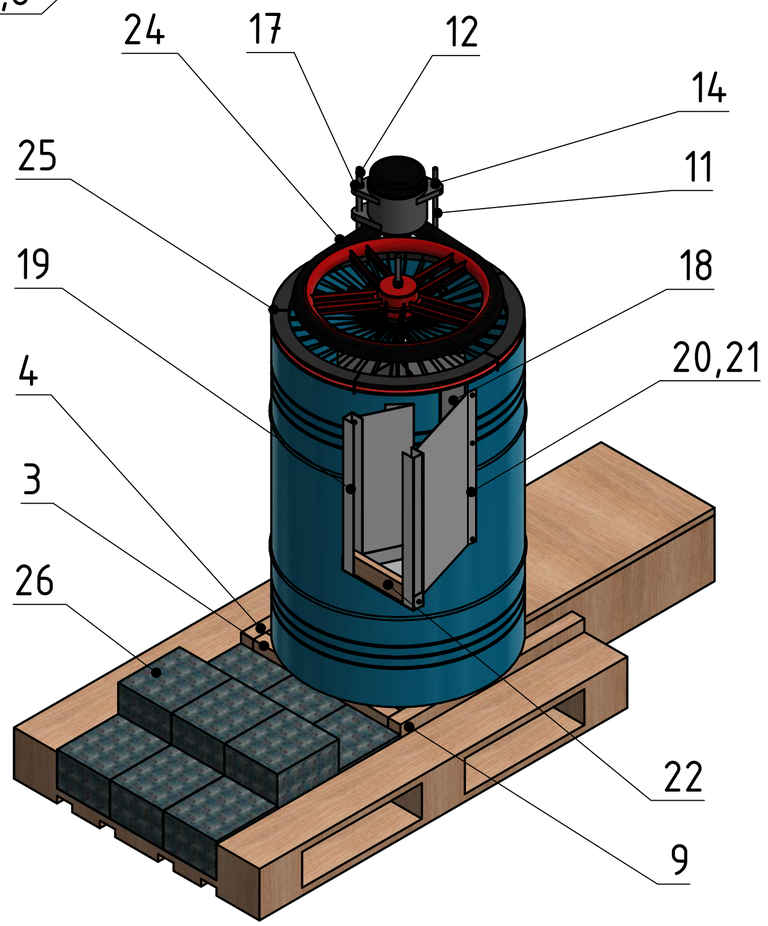

Position	Amount	Material	Description	Dimension
26	as needed	Stone	Stones	
25	1	Steel	Steel wire	ø0.8x3000
24	1	Rubber	Inner tube	16inch
23	1	-	Car alternator	
22	as needed	Wood	Wooden plate	20x100x210
21	18	Steel	Nuts	M4
20	18	Steel	Screws	M4x15
19	1	Aluminum	Aluminum plate	1.2x700x700
18	5	Steel	Steel plate	2x150x760
17	8	Steel	Nuts	M12
16	1	Aluminum	Motorcycle rim	16inch
15	1	-	Bicycle wheel	ø584
14	12	Steel	Nuts	M10
13	8	Steel	Screws	M10x35
12	1	Steel	Threaded rod	M12x1000
11	1	Steel	Threaded rod	M10x1000
10	4	Steel	Steel plate	2x40x100
9	22	Steel	Woodenscrews	ø4x50
8	1	Aluminum	Aluminum plate	1x370x495
7	1	Wood	Wooden plate	25x370x620
6	2	Wood	Wooden plate	25x140x970
5	1	Wood	Wooden plate	25x140x370
4	2	Wood	Wooden beam	40x140x600
3	1	Wood	Wooden beam	40x140x440
2	1	Steel	Oil barrel 200l	ø585x880
1	1	Wood	Wooden pallet	145x800x1200

		Datum	Name
Gezeichnet		24.11.2020	Jonas Ritz
Kontrolliert			
Norm			

Total assembly group

1

A2

Status	Änderungen	Datum	Name

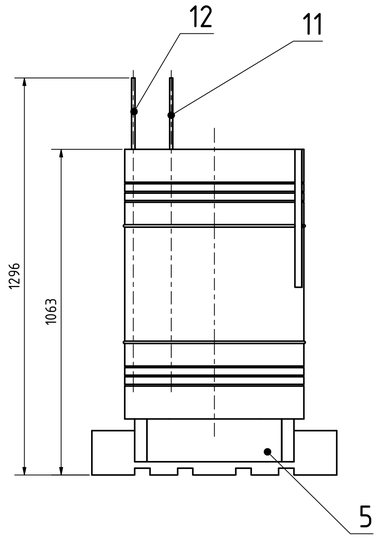

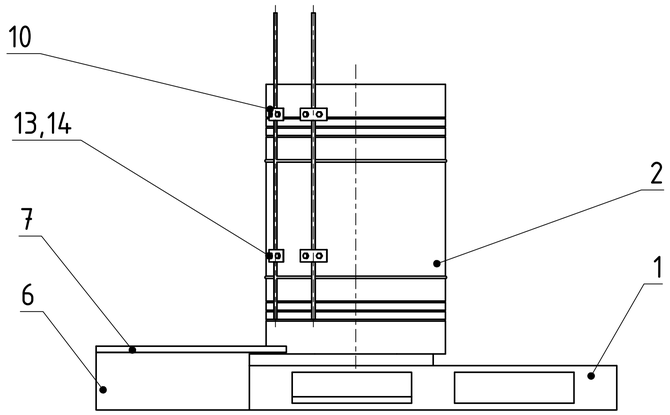

2,10,11,12,13,14

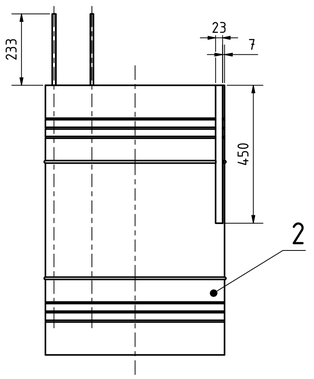

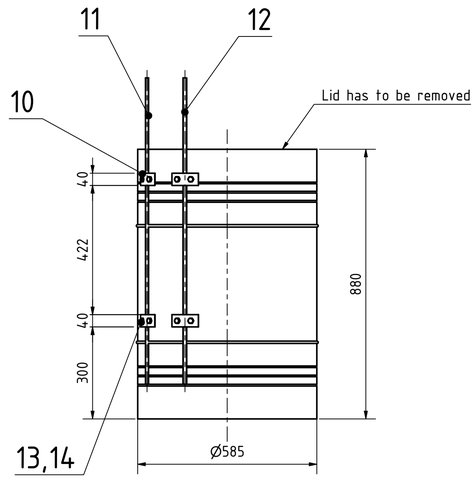

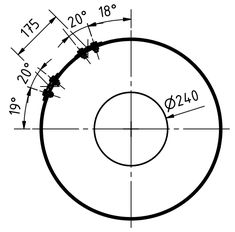

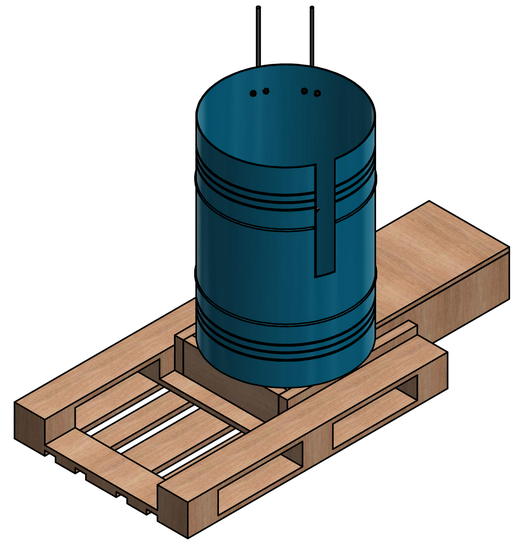

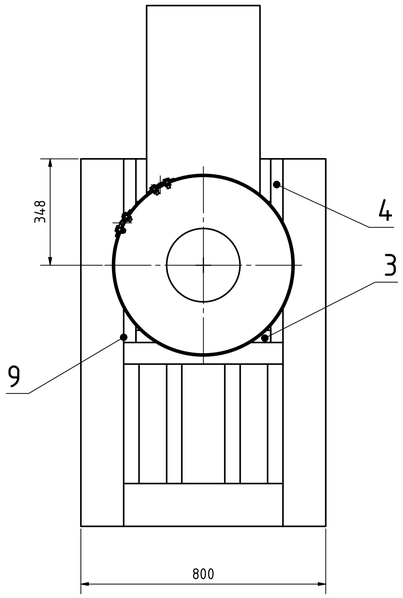

1,3,4,5,6,7,8

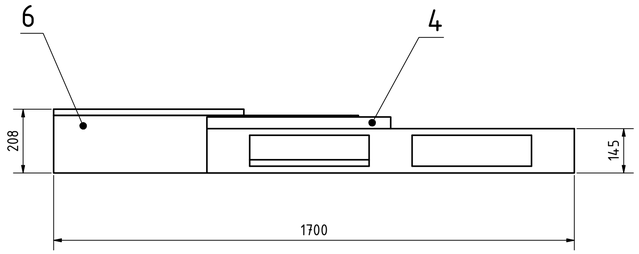

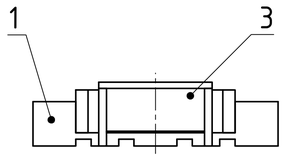

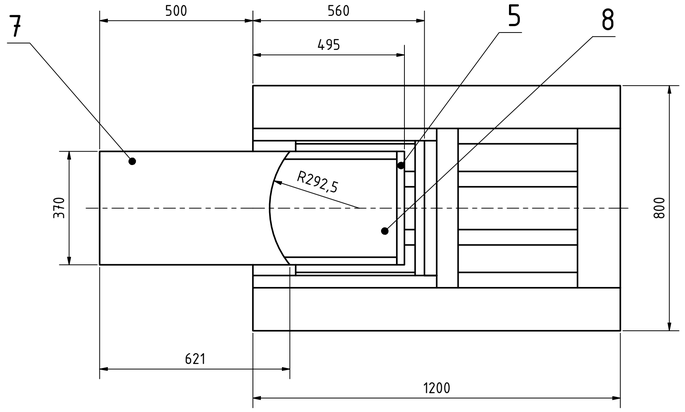

Position	Amount	Material	Description	Dimension
14	8	Steel	Nuts	M10
13	8	Steel	Screws	M10x35
12	1	Steel	Threaded rod	M12x1000
11	1	Steel	Threaded rod	M10x1000
10	4	Steel	Steel plate	2x40x100
9	22	Steel	Woodenscrews	ø4x50
8	1	Aluminum	Aluminum plate	1x370x495
7	1	Wood	Wooden plate	25x370x620
6	2	Wood	Wooden plate	25x140x970
5	1	Wood	Wooden plate	25x140x370
4	2	Wood	Wooden beam	40x140x600
3	1	Wood	Wooden beam	40x140x440
2	1	Steel	Oil barrel 200l	ø585x880
1	1	Wood	Wooden pallet	145x800x1200

	Datum	Name
Gezeichnet	24.11.2020	Jonas Ritz
Kontrolliert		
Norm		

Assembly group 1

1

A1

Status | Änderungen | Datum | Name

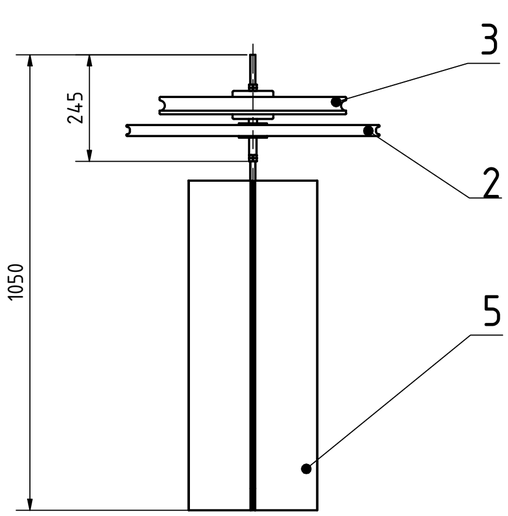

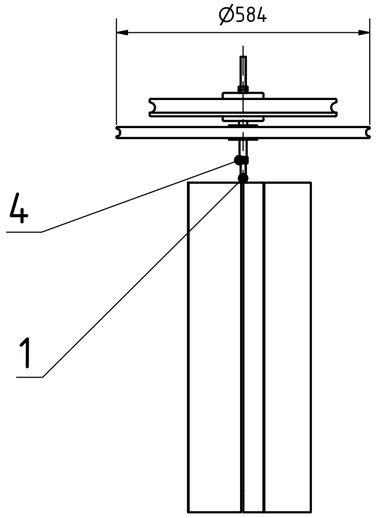

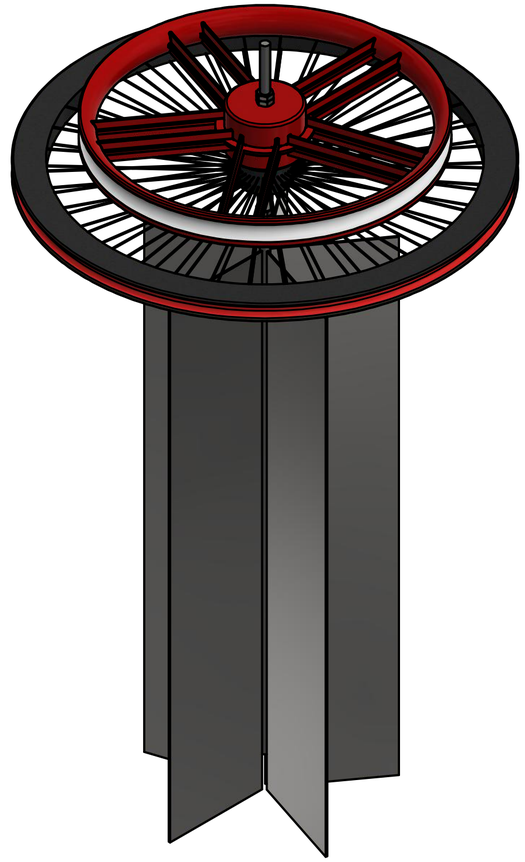

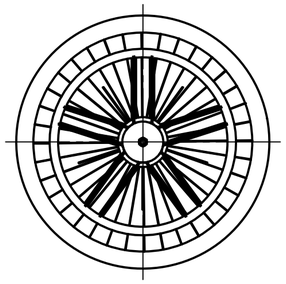

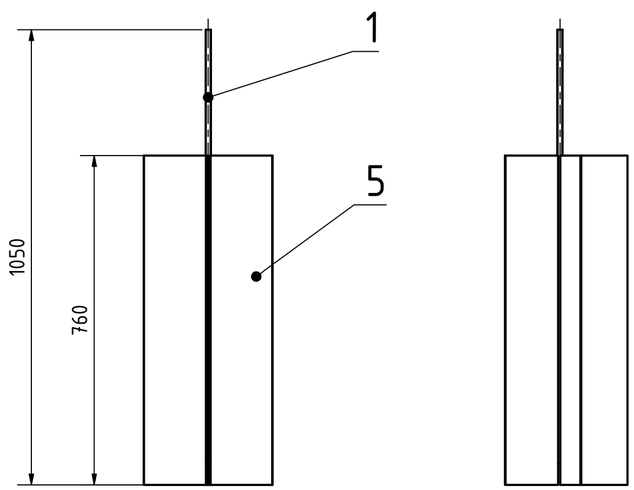

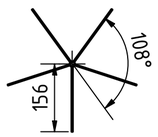

Position	Amount	Material	Description	Dimension
5	5	Steel	Steel plate	2x150x760
4	4	Steel	Nuts	M12
3	1	Aluminum	Motorcycle rim	16inch
2	1	-	Bicycle wheel	ø584
1	1	Steel	Threaded rod	M12x1000

	Datum	Name
Gezeichnet	25.11.2020	Jonas Ritz
Kontrolliert		
Norm		

Assembly group 2

1

A2

Status	Änderungen	Datum	Name

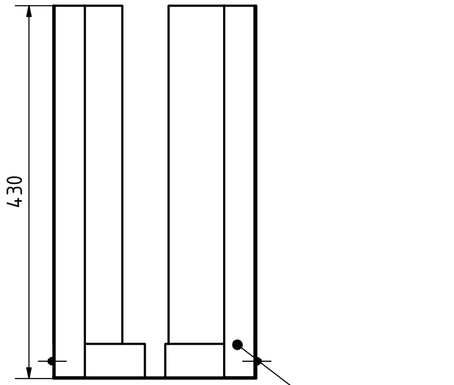

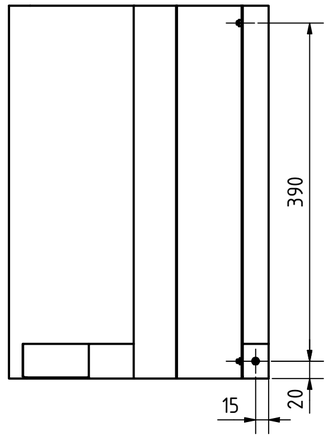

2

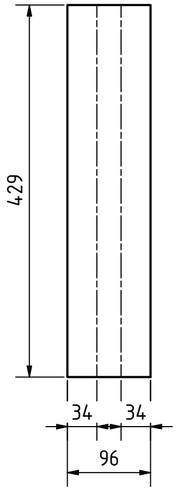

3

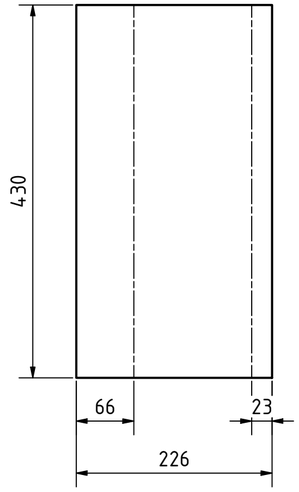

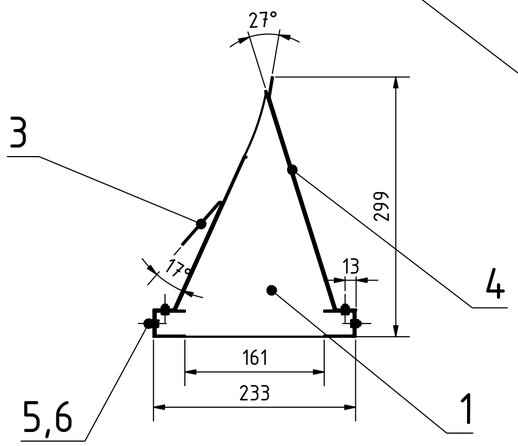

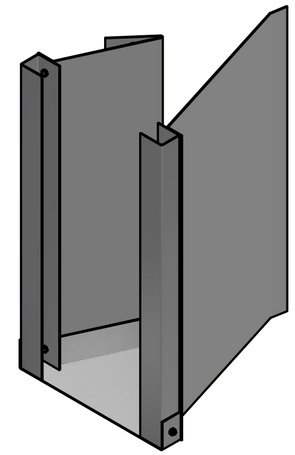

1

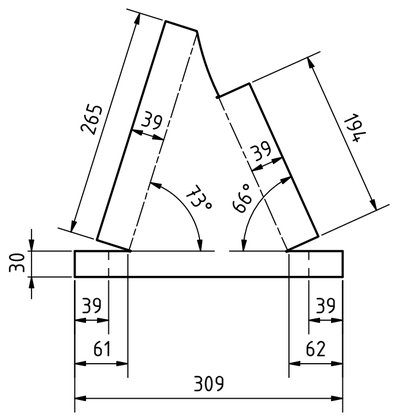

4

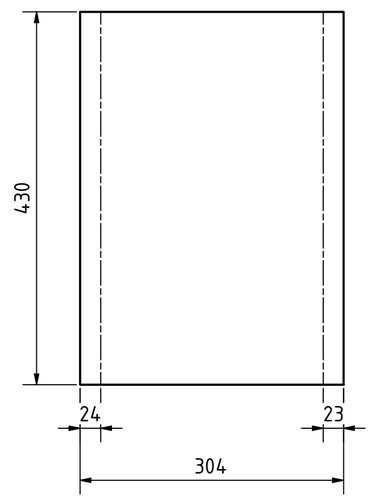

Position	Amount	Material	Description	Dimension
6	6	Steel	Nuts	M10
5	6	Steel	Screws	M10x10
4	1	Aluminum	Aluminum plate	1.2x304x430
3	1	Aluminum	Aluminum plate	1.2x126x430
2	2	Aluminum	Aluminum plate	1.2x96x429
1	1	Aluminum	Aluminum plate	1.2x295x309

	Datum	Name
Gezeichnet	24.11.2020	Jonas Ritz
Kontrolliert		
Norm		

Assembly group 3

1

A2

Status	Änderungen	Datum	Name